Response to the referees

Dear Kees Jan van Groenigen,

In the following document we comment on and explain how we address the issues and comments raised by the two referees. We found the comments of the referees very useful in highlighting important points, missing in the original manuscript. We will take the raised issues into account and adjust the manuscript accordingly. We are grateful and appreciate the two referees for their comments which we believe leads to an improved version of the manuscript.

Thank you for the consideration,

Response to referee comment # 1

General comments:

The study by Winther et al. presents continuous measurements of nitrous oxide isotopomers at concentration levels close to ambient and intends to determine isotope effects for two different bacterial organisms. Especially the endeavour to bring such measurements towards ambient concentration levels is valuable for the scientific community. In this context, this paper is of interest for the broad audience Biogeosciences attracts. There are some flaws, such as 1. The initial NO_3^- isotopic composition had to be estimated. 2. There is no nitrate balance provided, which would be helpful with regard to constraining f. 3. Concentration of other products, such as NO have not been accounted for. However, the manuscript provides some interesting calculation approaches, and the experiments involving P. chlororaphis are straightforward. All in all, I recommend acceptance for publication after addressing the below comments.

Specific comments:

See some more detailed comments below.

Title ok

Highlights Not given

Abstract P1, L10: Please specify the sentence “the continuous analysis of . . .”. The meaning is unclear without knowing the manuscript.

The sentence has been changed to “the continuous measurements of …”. (New version P.1, L10-11).

Please change reveal to reveals.

The spelling error has been corrected. (New version P.1, L11).

Introduction P2, L19: please change to positions, instead of position.

The spelling error has been corrected. (New version P.2, L18).

The objectives and the added value of another experiment on fractionation factors could be more to the point.
We added a phrase at the end of the introduction. “Isotope effects during denitrification are diverse and species dependent (e.g. Denk et al., 2017). Our study demonstrates a new way to determine fractionation factors from continuous measurements of N_2O.” (New version P.3, L23-24).

Materials and Methods P4, L12 and following: I suggest changing “before” to “upstream of”.
Agreed and changed. (New version P.4, L11).

In addition, the text does not comply with Figure1. From Figure 1, it seems like a Nafion and a Magnesium perchlorate / Ascarite trap was used. The Nafion reduces the water vapor to a certain dewpoint (please specity) and the magnesium perchlorate $Mg(ClO_4)_2$! removes the remaining water chemically. The Ascarite (this is not $Mg(ClO_4)_2$, but sodium hydroxide coated silica!!) removes the CO2!. This section needs to be corrected.
We agree that the description is incorrect and changed accordingly to: “Before the analyzer, a Nafion unit and an Ascarite trap is installed. The Nafion unit removes the bulk of H_2O vapor. Remaining water vapor is removed chemically by magnesium perchlorate ($Mg(ClO_4)_2$) in front and after the Ascarite (NaOH) section of the trap.” (New version P.4, L11-14).

P6, L1: the subsection head number is 2.4.1, but there is no 2.4.2, which does not make sense. I suggest numbering the subsection head to 2.5
Head number has been changed. (New version P.6, L1).

P7, L20: please change results to result
The spelling error has been corrected. (New version P.7, L20).

L7,P19/20: with regard to the reference to the supplementary, I suggest changing “unreacted” to “reacted” in P4,L14 of the supplementary (“. . .can therefore be calculated as the sum of the immediate product calculated for all reacted fractions of the substrate”), as the accumulated product is the result of the reacted fractions of the substrate.
We agree that the formulation is confusing and simplify to: “…be calculated as the sum of the respective immediate products.” (New supplementary version P.4, L14).

P8, (8): The numerator terms are quite clear, the denominator term is not required to my understanding. Please clarify.
We verified and the mass balance is correct.

P8, L26: Please change to net production.
We agree and corrections has been made accordingly. (New version P.8, L26).

P8, L30: This assumption is not in agreement with your expectations given on P3, L16-20. There it is assumed that $\delta^{15}N^{\alpha}$ becomes enriched (I agree with this assumption). In general, all N_2O isotopic species should become enriched in a situation in which only reduction occurs, as N_2O is the

substrate in this case, and a normal isotope effect occurs. However, this is not the case in Figures 6A/B. Please comment.
We see the origin of the confusion. The outcome of our analysis for *P. fluorescens* is indeed conflicting with the expectation given on P3, L16-20. This is obvious in Figure 6A/B and discussed later in the manuscript. On P8, L30 we only define the start of reduction for determining the fractionation coefficient. The bracket stating "(assumption based on reduction…)" is misleading and we removed it.

P9, L5: the fractionation factor during reduction is varied between 1 and 2, this means only not-normal isotope effects are allowed for the reduction of N_2O. A recent review on isotope effects in the N cycle, Denk et al. 2017 in Soil Biol. Biochem. (The nitrogen cycle: A review of isotope effects and isotope modeling approaches), shows that the literature has reported that N_2O reduction is associated with a normal isotope effect for $\delta^{15}N^{bulk}$. Please comment why this limitation was necessary.
We apologize, this is a typo. The reduction fractionation factor was varied between 0 and 2 which includes all possible isotope effects. Corrected. (New version P.9, L5).

Results Discussion P11, L2: The statement that the production rate is 10 times higher for P. Chlororaphis is ambiguous, since a net rate is compared to a "gross" rate (assuming direct conversion of NO_3^- to N_2O). Please add this to your interpretation that reaction rate cannot account for the difference in isotopic fractionation alone.
The reviewer is correct. We changed "production" to "net production". (New version P.11, L2).

P11, L15-17: This is pertinent information. Thank you. I only suggest to change the numbering from 1) and 2) for the results of the DNA comparisons to i) and ii). I was a little confused with the (1)-(4) numbering.
We agree and have changed accordingly. (New version P.11, L16).

Response to referee comment # 2

The manuscript of Malte Winther et al. describes the real-time analysis of site-specific N_2O isotopic composition from two denitrifying bacterial strains with a novel Picarro CRDS analyser. A setup for a closed-loop experiment was designed and applied in a number of prototype experiments. A correction function was developed for the spectrometer raw data and a modified Rayleigh model applied to derive fractionation factors.
The manuscript is an important contribution to research on N_2O isotopes and therefore of interest for a number of readers of Biogeosciences. The presented interpretation of singular incubation experiments might be questionable; at least given the "surprising" results, e.g. for ε_{SP} of N_2O reduction. But the manuscript should still be accepted after a number of minor revisions as detailed below:

Page 1 Line 8: The main application of the instrument might be for biogeochemical applications, e.g. soil sciences, at enhanced concentrations and not for atmospheric chemistry.
We agree that the manuscript would be good in soil sciences as well.

Page 1 Line 10 – 11: The expression "… reveal the transient pattern" is incomplete.
Changed to: "The continuous analysis of N_2O isotopomers reveals the transient isotope exchange between KNO_3, N_2O, and N_2." (New version P.1, L10-11).

Page 1 Line 15 – 17: The explanation for the SP isotopic fractionation for N_2O reduction above zero, "diffusive isotopic fractionation and a difference in active enzymes during production of N_2O", is not convincing.
We remove the statement (see also our comment to Page 12 Line 26).

Page 2 Line 18 – 19: Please rephrase the sentence "The position in the N_2O molecule are named …" to "N_2O molecules with ^{15}N substitution in the central or terminal position are named $^{15}N^{\alpha}$ for $^{14}N^{15}N^{16}O$ or $^{15}N^{\beta}$ for $^{15}N^{14}N^{16}O$, respectively."
The suggested correction is incorrect. Since it is the positions of the N atom which defines the name, and not the molecule. Changed to: "The positions in the N_2O molecule have been named N^{α} and N^{β} or short α and β (Yoshida and Toyoda, 2000). N_2O molecules with ^{15}N substitution in the central or terminal position are named $^{15}N^{\alpha}$ for $^{14}N^{15}N^{16}O$ or $^{15}N^{\beta}$ for $^{15}N^{14}N^{16}O$, respectively." (New version P.2, L16-19).

Page 2 Line 25: Please rephrase the expression to "… to enable continuous and selective measurements of the isotopomer abundances."
Correction has been applied. (New version P.2, L24).

Page 3 Line 4 – 6: The sentences "The primary anthropogenic sources of N_2O are organic and inorganic N fertilizers used for agriculture. The natural sources are primarily nitrification and denitrification in terrestrial and aquatic ecosystems." are misleading as the biotic (and abiotic) source processes for anthropogenic and natural N_2O emissions are similar, but anthropogenic emissions are enhanced due to fertilizer application. Please rephrase the sentences.
The sentences has been corrected. Now it reads "The primary anthropogenic increase in N_2O emission originate from organic and inorganic N fertilizers used for agriculture. The natural sources are primarily nitrification and denitrification in terrestrial and aquatic ecosystems." (New version P.3, L1-3).

Page 3 Line 17 – 18: The expression "… , the cleavage of N_2O is expected to have an increased fractionation effect on $^{15}N^{\alpha}$, due to …" might be rephrased to "the cleavage of N_2O is expected to fractionate in favor of the $^{15}N^{\alpha}$ molecule, due to …".
We adapt the suggestion and changed accordingly. (New version P.3, L14-15).

Page 3 Line 17 – 19: The statement that "diffusion into the cell (Tilsner et al., 2003) and enzymatic reduction (Wrage et al., 2004)" might be deleted.
These introductory statements line out what ideas have been presented to explain changes in SP. We would like to keep them.

Page 4 Line 8: The phrase "by placing the sample delivery system … in a closed loop" might be rephrased to "by a closed-loop gas flow through the …".
We adapt the suggestion and changed accordingly. (New version P.4, L8).

Page 4 Line 13: $Mg(ClO_4)_2$ is the chemical formula for Magnesiumperchlorate used for drying the measuring gas, but not for Ascarite used for removing CO_2. The scheme in Figure 1 shows the

correct setup of the trap.
We agree and the correction has been made accordingly. Also see comments to referee #1. (New version P.4, L11-14).

Page 4 Line 22 – 29: Please re-write this section, as the same information, that a concentration dependent correction for delta values is needed is given several times.
We removed duplicate statements from the section and write now: "Isotopomer measurements made with the G5101i-CIC have a N_2O concentration dependence and need to be corrected. There is a 1/concentration dependence, caused by small offsets in the measurement of the $^{14}N^{15}N^{16}O$ and $^{15}N^{14}N^{16}O$ peaks. These offsets are caused by baseline ripple created by optical cavity etalons. An etalon is an optical effect in which a beam of light undergoes multiple reflections between two reflecting surfaces, and whose resulting optical transmission or reflection is periodic in wavelength. The ripples are not always constant in phase, which means that the ripples can shift spectrally, which can cause the offset to drift over time. Because baseline ripple effects become more dominant as N_2O concentration decreases, the offset is largest at low concentrations." (New version P.4, L22-28).

Page 5 Line 5: The section on the O_2 correction (now Page 6 Line 18 – 23) could better be placed here.
The O_2 correction is related to the calibration gases we use for the specific experiments introduced on page 6. Therefore we prefer to leave it where it is. Moving the section to page 5 would lead to repeating the arguments on page 6.

Page 5 Section calibration gases (Table 1): Please check whether there is a mistake in the mean values in Table 1, e.g. the mean of 1.34, 1.08, 2.62 is not 1.32.
The mean values in Table 1 is not the mean of the three numbers, but rather the combined mean values, which depends on the number of measurements performed. That is the reason for the difference. That we use the combined mean values has been clarified.

Page 7 Line 6: The statement to give $\delta^{15}N^{\alpha}$ and $\delta^{15}N^{\beta}$ values for KNO_3 is wrong or at least a misunderstanding.
We agree that the way we phrased is misleading and reformulated to clarify the link between $\delta^{15}N^{\alpha}$, $\delta^{15}N^{\beta}$ and the isotopic composition of KNO_3: "The initial isotopic composition of KNO_3 calculates as the average of the end values for $\delta^{15}N^{\alpha}$ and $\delta^{15}N^{\beta}$ to -3.08 ‰ ± 1.05 (identical to the $\delta^{15}N^{bulk}$ value)." (New version P.7, L5-7).

Page 12 Line 3: The statement that differences in net production rates affect ε_{SP} seems questionable.
We agree and also write earlier in the manuscript that net production differences account for less than 10% of the effect. We now write: "We hypothesize that the slight difference in ε_{SP} originates predominantly from 4) fractionation associated with nitrous oxide reductase in *P. fluorescens*." (New version P.12, L5-6).

Page 12 Line 26: The statement that higher ε_{SP} values as reported in literature could be rationalized by diffusive isotope fractionation seems questionable, as diffusion is generally assumed to not affect the N_2O SP.
We agree that diffusive isotope fractionation is mass dependent and therefore has no effect on SP. Rereading the section we realize that the reduction part of Figure 7 is not fully described and would

therefore like to slightly adjust the phrasing. As to the statement in question it is misplaced and we remove it. The paragraph now reads: "A number of studies have investigated N_2O reduction from denitrification in soils (e.g. (Well and Flessa, 2009b; Köster et al., 2013a; Lewicka-Szczebak et al., 2014, 2015)). The results are only partly in accord with our findings for specific bacteria strains. While our results for ε_{bulk} are within the range of their findings, they find consistently negative ε_{SP} values while our results are generally positive. The only study on pure bacteria we know of is from Ostrom et al. (2007) for two bacteria strains different from ours namely *P. stutzeri* and *P. denitrificans*. They found ε_{SP} values between -6.8 ‰ and -5 ‰. At this point we have no explanation for the discrepancy but can find no artifact in our incubation setup." (New version P.12, L23-28).

Page 13 Line 2: The term "isotope depletion" is incomplete, it should be mentioned which isotopic species is depleted.

We agree and have adapted the formulation. Now we write "… find a bulk isotope depletion." (New version P.13, L4).

Continuous measurements of nitrous oxide isotopomers during incubation experiments

Malte Winther[1], David Balslev-Harder[1,2], Søren Christensen[3], Anders Priemé[4,5], Bo Elberling[5], Eric Crosson[6], and Thomas Blunier[1]

[1]Centre for Ice and Climate, Niels Bohr Institute, University of Copenhagen, Denmark
[2]DFM - Danish National Metrology Institute, Kgs. Lyngby, Denmark
[3]Section for Terrestrial Ecology, Department of Biology, University of Copenhagen, Denmark
[4]Section for Microbiology, Department of Biology, University of Copenhagen, Denmark
[5]Center for Permafrost, Department of Geosciences and Natural Resource Management, University of Copenhagen, Denmark
[6]Picarro Inc, Santa Clara, CA 95054 USA

Correspondence to: Malte Winther (malte.winther@nbi.ku.dk)

Abstract. Nitrous oxide (N_2O) is an important and strong greenhouse gas in the atmosphere. It is produced by microbes during nitrification and denitrification in terrestrial and aquatic ecosystems. The main sinks for N_2O are turnover by denitrification and photolysis and photo-oxidation in the stratosphere. In the linear N=N=O molecule ^{15}N substitution is possible in two distinct positions, central and terminal. The respective molecules, $^{14}N^{15}N^{16}O$ and $^{15}N^{14}N^{16}O$, are called isotopomers. It has been demonstrated that N_2O produced by nitrifying or denitrifying microbes exhibits a different relative abundance of the isotopomers. Therefore, measurements of the site preference (difference in the abundance of the two isotopomers) in N_2O can be used to determine the source of N_2O i.e. nitrification or denitrification. Recent instrument development allows for continuous position dependent $\delta^{15}N$ measurements at N_2O concentrations relevant for studies of atmospheric chemistry. We present results from continuous incubation experiments with denitrifying bacteria, *Pseudomonas fluorescens* (producing and reducing N_2O) and *Pseudomonas chlororaphis* (only producing N_2O). The continuous measurements of N_2O isotopomers reveals the transient isotope exchange between KNO_3, N_2O, and N_2. We find bulk isotopic fractionation of -5.01 ‰ ± 1.20 for *P. chlororaphis*, in line with previous results for production from denitrification. For *P. fluorescens*, the bulk isotopic fractionation during production of N_2O is -52.21 ‰ ± 9.28 and 8.77 ‰ ± 4.49 during N_2O reduction.

The SP isotopic fractionation for *P. chlororaphis* is -3.42 ‰ ± 1.69. For *P. fluorescens*, the calculations result in SP isotopic fractionation values of 5.73 ‰ ± 5.26 during production of N_2O and 2.41 ‰ ± 3.04 during reduction of N_2O. In summary, we implemented continuous measurements of N_2O isotopomers during incubation of denitrifying bacteria and believe that similar experiments will lead to a better understanding of denitrifying bacteria and N_2O turnover in soils and sediments and ultimately hands-on knowledge on the biotic mechanisms behind greenhouse gas exchange of the globe.

Keywords

Nitrous oxide, isotopomers, site preference, greenhouse gas, denitrification, *Pseudomonas fluorescens*, *Pseudomonas chlororaphis*

1 Introduction

The atmospheric concentration of nitrous oxide (N_2O) has increased from approximately 271 ppb before the industrialization to 324 ppb in 2011 (Ciais et al., 2013). This increase has resulted in (1) N_2O being the third most important greenhouse gas, that is N_2O has the third highest contribution to the radiative forcing of the naturally occurring greenhouse gases (Hartmann et al., 2013), and (2) an increased production of nitrogen oxides (NOx) in the stratosphere and thereby an increased ozone-depletion (Forster et al., 2007; Kim and Craig, 1993).

Ice core records show that N_2O concentrations positively correlate with northern hemispheric temperature variations, e.g. during the last glacial-interglacial termination as well as over the rapid climate variations occurring during the glacial period, known as Dansgaard-Oeschger events (D-O events) (Schilt et al., 2010). However, occasionally (e.g. D-O event 15 and 17) the N_2O concentration increases long before the onset of the dramatic temperature change (Schilt et al., 2010), providing a potential early warning for rapid climate change. Isotopomers of N_2O provide information on the sources (Pérez et al., 2000, 2001; Park et al., 2011) i.e. whether N_2O originates predominately from nitrification or denitrification processes. As the conditions/ circumstances leading to emissions from the two processes differ both for the marine and terrestrial sources measuring isotopomers potentially improves our understanding of the climate conditions leading to the release of N_2O over rapid climatic changes.

The N_2O molecule has an asymmetric linear structure (N=N=O) where the position of the ^{15}N can be discriminated. The positions in the N_2O molecule have been named N^α and N^β or short α and β (Yoshida and Toyoda, 2000). N_2O molecules with ^{15}N substitution in the central and terminal positions are named $^{15}N^\alpha$ for $^{14}N^{15}N^{16}O$ or $^{15}N^\beta$ for $^{15}N^{14}N^{16}O$, respectively. The two isotopomers can be distinguished by isotope ratio mass spectrometry, if measurements of the NO fragment are included. A distinction is furthermore possible using mid-infrared spectroscopy because the rotational and vibrational conditions are different for the two isotopomers providing spectral regions where absorptions of the two isotopomers do not overlap (Waechter et al., 2008; Mohn et al., 2010, 2012; Köster et al., 2013b; Heil et al., 2014). For isotopomer measurements at low N_2O concentration (low ppm range), a joint instrument development was executed, applying cavity ring down spectroscopy (CRDS) to enable continuous and selective measurements of the isotopomer abundances.

The isotopic composition of a sample is reported as delta values which represents the deviation of the elemental isotope ratio R_{sample} in the sample from a standard R_{std} (Eq. 1). Delta values can be calculated for bulk N_2O as well as for $\delta^{15}N^\alpha$ and $\delta^{15}N^\beta$. All results are reported relative to the isotopic composition of atmospheric nitrogen.

$$\delta^{15}N = \frac{R_{Sample}}{R_{Std}} - 1 \quad \text{where} \quad R = \frac{[^{15}N]}{[^{14}N]} \tag{1}$$

The N_2O bulk isotopic composition calculates as the average of $\delta^{15}N^\alpha$ and $\delta^{15}N^\beta$ (Eq. 2) while the site preference (SP) is by definition their difference (Eq. 2) (Brenninkmeijer and Röckmann, 1999; Toyoda et al., 2002).

$$SP = \delta^{15}N^\alpha - \delta^{15}N^\beta \quad , \quad \delta^{15}N^{bulk} = \frac{\delta^{15}N^\alpha + \delta^{15}N^\beta}{2} \tag{2}$$

There are multiple natural and anthropogenic sources of N_2O. The primary anthropogenic increase in N_2O emission originate from organic and inorganic N fertilizers used for agriculture. The natural sources are primarily nitrification and denitrification in terrestrial and aquatic ecosystems (Mosier et al., 1998; Olivier et al., 1998).

Denitrification is a stepwise biological reduction process in which denitrifying bacteria ultimately produce nitrogen (N_2). Under anaerobic conditions the denitrifying bacteria use nitrate (NO_3^-) instead of oxygen as an electron acceptor in the respiration of organic matter. Through multiple anaerobic reactions N_2 is produced as the end product of the complete denitrifying process (reaction R1) (Firestone and Davidson, 1989).

$$NO_3^- \rightarrow NO_2^- \rightarrow NO \rightarrow N_2O \rightarrow N_2 \tag{R1}$$

Each of these anaerobic reactions is carried out by a genuine enzyme, i.e., the production of N_2O is caused by the reaction between nitric oxide (NO) and the enzyme nitric oxide reductase (NOR). The NOR enzyme works as a catalyst in the reduction of NO as shown in reaction R2 (Wrage et al., 2001; Tosha and Shiro, 2013).

$$2NO + 2e^- + 2H^+ \rightarrow N_2O + H_2O \tag{R2}$$

The cleavage of the covalent N=O bond of N_2O leading to N_2 and H_2O is the result of N_2O reduction during bacterial denitrification (R3). According to kinetic isotope theory, the cleavage of N_2O is expected to fractionate in favor of the $^{15}N^{\alpha}$ molecule, due to a stronger $^{15}N-O$ bond compared to the $^{14}N-O$ (Popp et al., 2002), diffusion into the cell (Tilsner et al., 2003), and enzymatic reduction (Wrage et al., 2004). N_2O reduction during bacterial denitrification is therefore expected to lead to an increase in SP.

$$N_2O + 2e^- + 2H^+ \rightarrow N_2 + H_2O \tag{R3}$$

Reactions with different enzymes typically result in specific isotopic fractionation. The isotopic composition of the intermediately produced N_2O during denitrification is a consequence of multiple reaction steps. Two species of denitrifying bacteria with slightly different enzymes potentially leads to different fractionation. In this study, we compared the fractionation of two contrasting denitrifying bacteria; *Pseudomonas fluorescens* producing and reducing N_2O, and *Pseudomonas chlororaphis* producing but not reducing N_2O. Isotope effects during denitrification are diverse and species dependent (e.g. Denk et al. (2017)). Our study demonstrates a new way to determine fractionation factors from continuous measurements of N_2O.

2 Method

Our objective was to perform continuous position dependent $\delta^{15}N$ measurements of two different bacterial cultures during incubation experiments. Using two denitrifying bacterial cultures we determined the isotopic fractionation and SP during production and reduction of N_2O, respectively.

2.1 Instrumentation

Bacterial production of N_2O was continuously measured by mid-infrared cavity ringdown spectroscopy using a prototype of the Picarro G5101-i analyzer (in the following named G5101i-CIC) (Picarro, Santa Clara, California, USA). The measurements are non-destructive and are therefore suitable for incubation experiments. The CRDS instrument measures the $^{14}N^{14}N^{16}O$, $^{15}N^{\alpha}$ and $^{15}N^{\beta}$ absorption features of N_2O in the wavelength region between 2187.4 cm^{-1} and 2188 cm^{-1} (Balslev-Clausen, 2011). The typical precision of the instrument over 10 minutes averaging is < 0.3 ppb for the N_2O mixing ratio and < 0.4 ‰ for each of the delta values of the isotopomers for concentrations in the range of 200 ppb – 2000 ppb.

Measurements are made by a closed-loop gas flow through the G5101i-CIC with a microbial incubation glass chamber (Fig. 1). Circulation is provided by a leak-reduced diaphragm pump installed downstream from the analyzer. The pump (KNF N84.4 ANE) has been sealed using vacuum sealant (Celvaseal high vacuum leak sealant, Myers vacuum repair service, Inc., Kittanning, PA 16201, USA). A low leak rate is prerequisite for accurate measurements in a closed loop experiment. Upstream of the analyzer, a Nafion unit and an Ascarite trap is installed. The Nafion unit removes the bulk of H_2O vapor. Remaining water vapor is removed chemically by magnesium perchlorate($Mg(ClO_4)_2$) in front and after the Ascarite ($NaOH$) section of the trap. Both gases are removed to exclude potential spectral interference with N_2O in the cavity of the analyzer. Underneath the glass chamber a magnetic stirrer is installed. The stirrer serves two purposes 1) ensure a complete mixing of the bacterial solution and the added nutrient, i.e. potassium nitrate (KNO_3^-), and 2) facilitate gas exchange.

In addition to the measuring mode, the system can be flushed with N_2 (not shown in Fig. 1). The flushing mode is used to obtain an anaerobic starting point of the incubation experiment free of N_2O. The flushing procedure is fully automated to ensure reproducibility. The entire incubation setup is flushed with N_2 for 310 seconds at a high flow rate. The resulting overpressure in the incubator is released prior to switching back to the closed loop position.

2.2 Correction of CRDS concentration dependence

Isotopomer measurements made with the G5101i-CIC have a N_2O concentration dependence and need to be corrected. There is a 1/concentration dependence, caused by small offsets in the measurement of the $^{14}N^{15}N^{16}O$ and $^{15}N^{14}N^{16}O$ peaks. These offsets are caused by baseline ripple created by optical cavity etalons. An etalon is an optical effect in which a beam of light undergoes multiple reflections between two reflecting surfaces, and whose resulting optical transmission or reflection is periodic in wavelength. The ripples are not always constant in phase, which means that the ripples can shift spectrally, which can cause the offset to drift over time. Because baseline ripple effects become more dominant as N_2O concentration decreases, the offset is largest at low concentrations.

Fig. 2 shows results from seven dilution experiments where we gradually mixed a pure N_2O gas with a N_2/O_2 mixture (20.1 % O_2 and 79.9 % N_2, purity 99.999 %). Measurements were performed in a 60 minutes stepwise (18 steps) sequence of both increasing and decreasing concentrations (fig. 2).

We chose to fit the raw data with a cubic spline smoothing function (CSS-function) (Brumback and Rice, 1998). The best fit of these CSS-functions are found (using a smoothing parameter of p = 0.999) in a regression analysis. Four outliers were identified to be outside the 2σ boundary and were removed from the data set (the red circles in fig. 2). After these outliers were removed the best fit was found again (p = 0.999) and the concentration dependent correction was applied as shown with the green profiles in Fig. 2. Over the course of the experiments, no further instrumental drift was observed.

2.3 Calibration gases

Our working standards are CIC-MPI-1 and CIC-MPI-2, prepared based on two standard gases provided by J. Kaiser at University of East Anglia (UEA), Norwich, United Kingdom. These standard gases, MPI-1 and MPI-2, are pure N_2O gases with different isotopic composition (Kaiser, 2002). In our laboratory, each of the standard gases was diluted with a N_2/O_2 mixture (20.1 $\%$ O_2 and 79.9 $\%$ N_2, purity 99.999 $\%$) resulting in the two new standard gases, CIC-MPI-1 and CIC-MPI-2. We had both CIC-standard gases measured at four different laboratories to ensure consistent isotopic values (see Table 1). The gases were originally measured at University of East Anglia in Norwich, United Kingdom (UEA). After mixing the gases were measured three times using GC/IRMS measurements at Tokyo Institute of Technology in Japan. At Institute for Marine and Atmospheric research Utrecht in The Netherlands (IMAU) the gases were measured 22 times using GC/IRMS. At the Centre for Ice and Climate in Copenhagen Denmark (CIC) the gases were measured continuously over two hours. All measurements are reported relative to atmospheric N_2. The root-mean-square deviations (RMSD) calculated from the three laboratories with respect to the original UAE data (Table 1) are similar to the RMSD calculated by Mohn et al. (2014). They present RMSD calculations based on gas measurements performed at 12 different laboratories using both IRMS and laser spectroscopy.

2.4 Pure bacterial cultures

The two bacterial cultures used in this study are both gram-negative bacteria with the capability to denitrify, i.e. reduce nitrate to gaseous nitrogen. Isolates were obtained from an agricultural soil of sandy loam type (Roskilde Experimental Station) on 11 April 1983. One culture is a *Pseudomonas fluorescens*, bio-type D that reduces NO_3^- all the way to N_2. The second culture, *Pseudomonas chlororaphis*, is only capable of reducing NO_3^- to N_2O (Christensen and Bonde, 1985), which means that the nitrous oxide reductase is absent or at least not active in this organism. The latter bacterium is contained in the American Type Culture Collection with accession number ATCC 43928 (Christensen and Tiedje, 1988). The cultures were grown anoxic in 50 ml serum bottles with 1/10 tryptic soy broth (Difco) added 0.1 $g\ KNO_3 \cdot L^{-1}$. After six days of growth at room temperature (24°C), *P. chlororaphis* had converted all N in NO_3^- into N_2O. The bacterial culture of *P. Fluorescens* was cultivated for six days at a slightly lower temperature (15°C) to assure that the cultures were in a comparable phase of potential activity when assayed for gas production/reduction activity. The six days old cultures were used in the incubation experiment where it is conditional for the denitrifying process that organic carbon is available, that the concentration of oxygen is low, and that the concentration of NO_3^- is high (Wrage et al., 2001; Stuart Chapin III et al., 2002).

2.5 Bacterial incubation experiments

50 mL bacterial solution of *P. chlororaphis* or *P. fluorescens* was placed in a petri-dish in the 1000 mL incubation chamber. Hereafter, the setup was flushed with pure $\mathrm{N_2}$ (purity 99.9999 $\%$) to ensure anaerobic conditions. To ensure no $\mathrm{N_2O}$ gas exchange prior to the experiment, the bacterial solution was left for 90 minutes under constant magnetic stirring. Then the incubation chamber was opened and the bacterial solution was fed with 2.5 mL and 15 mL 0.45 mM $\mathrm{KNO_3}$ for *P. chlororaphis* and *P. fluorescens*, respectively. The incubation experiment started by again flushing the setup with pure $\mathrm{N_2}$ immediately after the addition of $\mathrm{KNO_3}$.

A total of seven replicate incubations of the full denitrifying bacteria (*P. fluorescens*) and five replicate incubations of the denitrifying bacteria with no active nitrous oxide reductase (*P. chlororaphis*) were executed. All of the cultures were continuously measured from the moment $\mathrm{KNO_3}$ was added to the bacterial incubations. We terminated experiments with *P. fluorescens* when the $\mathrm{N_2O}$ concentration was below 0.2 ppm. For *P. chlororaphis*, we defined the end of the experiment when the $\mathrm{N_2O}$ concentration had reached a constant level for 200 minutes.

Continuous measurements of the bacterial production of $\mathrm{N_2O}$ from *P. chlororaphis* were performed for approximately 500 minutes for each replica. All five replicas were measured within one week, starting at the same hour of the day and after equally long cultivation prior to the measurements. The bacterial evolution, of $\mathrm{N_2O}$ production and reduction, from *P. fluorescens* was continuously measured for about 1000 minutes. The seven replicas were measured during three one week measuring campaigns over the course of half a year, always with an equally long cultivation prior to measurements.

Our CIC-MPI standards contain $\mathrm{N_2O}$ in an $\mathrm{O_2/N_2}$ mixture while our incubation measurements were carried out in an $\mathrm{N_2}$ atmosphere. This difference has a significant effect on the spectroscopy. We find a linear dependence similar to the one found by (Erler et al., 2015). The presented data have been corrected for the effect, which is 15.27 ‰, 11.66 ‰, and 13.47 ‰ for $\delta^{15}N^{\alpha}$, $\delta^{15}N^{\beta}$, and $\delta^{15}N^{bulk}$ respectively (see supplementary). Given the leak rate of the system we estimate that the $\mathrm{O_2}$ concentration has not increased by more that 0.002 $\%$ over the course of the experiment. We therefore neglect the effect of a continuously increasing $\mathrm{O_2}$ concentration and assume a constant $\mathrm{O_2}$ concentration of 0 $\%$.

2.6 Determination of isotopic fractionation

Our incubation experiments are Rayleigh type experiments. In the following, we determine the underlying isotope fractionation from the isotopic evolutions in the incubator under this assumption. Rayleigh fractionation describes the changing isotopic composition in the substrate and product of a unidirectional one-step reaction. Lord Rayleigh (1896) derived the equation for the fractionating isotope ratio of the substrate (Eq. 3) as:

$$\frac{R_s}{R_{s,0}} = f^{\left(\alpha_{p/s}-1\right)} \tag{3}$$

where $R_{s,0}$ is the initial isotope ratio of the substrate, R_s is the isotope ratio of the substrate at time t, $\alpha_{p/s}$ is the fractionation factor of the product versus the substrate, and f is the unreacted fraction of substrate at time t. The corresponding equation for

the isotopic ratio of the accumulated product $R_{p,acc}$ derives as given in Eq. 4.

$$R_{p,acc} = R_{s,0} \cdot \left(\frac{1 - f^{\alpha_{p/s}}}{1 - f} \right) \tag{4}$$

The isotopic fractionation is defined as $\epsilon = \alpha$ - *1*. We do not know the isotopic composition of KNO_3 used for our experiments. However, when all KNO_3 has reacted to N_2O, its isotopic composition is identical to the initial composition of KNO_3. The final isotopic values of N_2O for *P. chlororaphis* can therefore be used to estimate the initial composition of KNO_3. The initial isotopic composition of KNO_3 calculated as the average of the end values for $\delta^{15}N^{\alpha}$ and $\delta^{15}N^{\beta}$ to -3.08 ‰ ± 1.05 (identical to the $\delta^{15}N^{bulk}$ value).

2.6.1 Fractionation associated with N_2O production

The fractionation associated with production of N_2O is the result of multiple reactions with various isotopic fractionations (Ostrom and Ostrom, 2011). Although, Ostrom and Ostrom (2011) argue that the fractionation observed during production of N_2O via reduction of NO_3^- can be treated as a net isotope effect with NO_3^- being the substrate and N_2O as the product. During production of N_2O Eq. 4 is therefore used in calculation of the net fractionation factor and the net isotope effect of $\delta^{15}N^{bulk}$. For the two isotopomers Eq. 4 needs to be slightly modified (see supplementary). The SP isotopic fractionation is derived using the relationship $\epsilon_{sp} = \epsilon_{\alpha} - \epsilon_{\beta}$ as stated by Ostrom et al. (2007) and Well and Flessa (2009a).

2.6.2 Modifications to the Rayleigh model

To describe the evolution of the isotopomers during production of N_2O, the Rayleigh process is not directly applicable to the isotopomers as the two isotopomers both are direct products of the same denitrification process from the same batch of denitrifying bacteria and nitrate. The accumulated product for the two isotopomers can be determined (as presented in the supplementary). The calculations result in an isotopomer correction factor φ_{α} and φ_{β} for the two isotopomers respectively.

$$\varphi_{\alpha} = \frac{\alpha_{\alpha}}{\alpha_{bulk}} \tag{5}$$

$$\varphi_{\beta} = \frac{\alpha_{\beta}}{\alpha_{bulk}} \tag{6}$$

The fractionation factor for the bulk is denoted α_{bulk}, while the fractionation factors for the two isotopomers are presented as α_{α} and α_{β}, respectively. The Rayleigh equation for the accumulated product of $\delta^{15}N^{\alpha}$ ($R^{\alpha}_{p,acc}$) is therefore as presented in Eq. 7, in which $R^{bulk}_{p,acc}$ is the accumulated product calculated for $\delta^{15}N^{bulk}$. A similar equation exists for $R^{\beta}_{p,acc}$, using $\delta^{15}N^{\beta}$ and φ_{β}:

$$R^{\alpha}_{p,acc} = R^{bulk}_{p,acc} \cdot \varphi_{\alpha} \tag{7}$$

Equation 7 is valid for *P. chlororaphis*. For *P. fluorescens*, both an immediate reduction and an uptake reduction take place simultaneously with N_2O production due to the pre-experimental cultivation leading to activation of all enzymes in the bacterial solution. Part of the freshly produced N_2O is therefore immediately reduced to N_2. This reduction is fractionating with fractionation factor α_{α}^{R}, α_{β}^{R}, and α_{bulk}^{R}, respectively for each of the isotopomers and the bulk. The isotope imprint of the reduction on the remaining N_2O depends on the ratio between reduction rate and production rate, from here on referred to as the reduction correction parameter (γ). Assuming γ is constant (for one experiment cf. Fig. 3B) results in the following first order approximation of the accumulated product including the isotope imprint of the reduction on the remaining N_2O ($R_{p,r}^{\alpha}$).

$$R_{p,r}^{\alpha} = \frac{R_{p,acc}^{\alpha} \cdot \left(1 - \alpha_{\alpha}^{R} \cdot \gamma\right)}{1 - \gamma} \tag{8}$$

Equation 8 is presented for $\delta^{15}N^{\alpha}$, though similar equations is used for both $\delta^{15}N^{\beta}$ and $\delta^{15}N^{bulk}$. For any calculated ratio the values are given in ‰ using the delta-notation (Eq. 1).

2.6.3 Isotopic fractionation associated with N_2O reduction

The isotopic fractionation during reduction of N_2O to N_2 derives from Eq. 3. Equation 3 is valid for the bulk ^{15}N / ^{14}N isotope ratios of N_2O ($\delta^{15}N^{bulk}$) and for both of the two isotopomer isotope ratios ($\delta^{15}N^{\alpha}$ and $\delta^{15}N^{\beta}$) (Mariotti et al., 1981; Menyailo and Hungate, 2006; Ostrom et al., 2007; Lewicka-Szczebak et al., 2014).

2.6.4 Fitting procedure

We determine the respective isotopic fractionation during production and reduction of N_2O for each of the bacterial strains assuming a Rayleigh type process. The best fit (highest R^2) is found using an iterative approach between the measured data and the Rayleigh fractionation model for the accumulated product.

For *P. chlororaphis* (being a pure producer of N_2O) we use Eq. 4 and 7 as the Rayleigh fractionation model for the $\delta^{15}N^{bulk}$ and the two isotopomers, respectively. We fit the Rayleigh fractionation model to the measured data. The highest R^2 values are iteratively found, using iterative determination of the fractionation factor during production of N_2O ($0 \leq \alpha \leq 1$). The limits of the unreacted fraction of the substrate (f) was set to $f_{start} = 1$ and $f_{end} = 0$.

Since N_2O is the product and the substrate for production and reduction respectively Eq. 8 and 3 are applied for *P. fluorescens* to the corresponding process. We defined the section of net production as being from the start of the measurements until the net production (net emission) rate turns negative. From the calculations of the net production rates (see Fig. 3) we believe that N_2O production continues after the point of maximum concentration. However, at one point NO_3^-, NO_2^- and NO are fully consumed and *P. fluorescens* is forced to exclusively reduce N_2O. We defined the start of the section where *P. fluorescens* is only reducing N_2O to the point where both $\delta^{15}N^{\alpha}$ and $\delta^{15}N^{\beta}$ start decreasing. Between the end of the net production and the start of the exclusive reduction, no Rayleigh model can be fitted.

The fractionation factors resulting in the highest R^2 values are picked as the best fit fractionation factor for each specific evolution. In the calculations of the N_2O production from *P. fluorescens* the fractionation factor during N_2O reduction is required. We therefore first fit the Rayleigh fractionation model (Eq. 3) to the measured N_2O reduction data. The highest R^2 values are iteratively found, using 1) the extremes of the unreacted fraction of the substrate being f_{start} = 1 and f_{end} = 0, 2) the fractionation factor during reduction of N_2O ($0 \leq \alpha \leq 2$). Secondly we fitted the Rayleigh fractionation model (Eq. 8) to the measured N_2O production data. The highest R^2 values are iteratively found by varying 1) the extremes of the unreacted fraction of the substrate (f_{start} and f_{end}) with $1 \leq f_{start} < f_{end} \leq 0$ as the boundary conditions, 2) the reduction correction parameter (γ) in the range $0 \leq \gamma \leq 1$, and 3) the fractionation factor during production of N_2O ($0 < \alpha < 1$), and using the fractionation factor during N_2O reduction (from calculations above).

Nitric oxide (NO) accumulation in the headspace can not be excluded from any of the presented N_2O production experiments. The effect of accumulation of NO in the headspace is assumed to be addressed by iterative determination of f_{end} and f_{start} (Table 4 and Table 2 for *P. chlororaphis* and for *P. fluorescens*, respectively), hence no further adjustment is taken.

3 Results

The evolution of N_2O concentration over time from the two bacterial strains shows two very distinctive patterns with both an increasing and decreasing N_2O concentration characteristic for *P. fluorescens* and an increasing N_2O concentration followed by a stabilization characteristic for *P. chlororaphis* (Fig. 3A) as has previously been described by Christensen and Tiedje (1988). These distinctive characteristics are only vaguely seen in the respective dynamics of the SP for the two bacterial strains (Fig. 4A and 4B).

3.1 Pseudomonas chlororaphis

Paralleling the increase in N_2O concentration (Fig. 3A), we also find an increase in $\delta^{15}N^{\alpha}$, $\delta^{15}N^{\beta}$ and $\delta^{15}N^{bulk}$ over time (Fig. 5A and 5B). The final product of *P. chlororaphis* is N_2O; this is a unidirectional transfer of nitrogen from KNO_3 to N_2O and thereby a Rayleigh process although multiple fractionations are involved. Figure 5A and 5B shows the best fit Rayleigh profile for $\delta^{15}N^{\alpha}$ and $\delta^{15}N^{\beta}$ respectively.

The modeled Rayleigh distillation profiles were found to match the production of N_2O from *P. chlororaphis* to a relatively high degree. The average coefficient of determination (R^2) between data and fitted Rayleigh curves are 72.15 %, 64.20 %, and 76.31 % for $\delta^{15}N^{\alpha}$, $\delta^{15}N^{\beta}$ and $\delta^{15}N^{bulk}$ respectively. The calculations of the isotopic fractionation for the fractionation of $\delta^{15}N^{\alpha}$ give a mean value of -6.72 ‰ $\pm$ 1.54 (Table 4). For $\delta^{15}N^{\beta}$ the mean isotopic fractionation was found to be -3.28 ‰ $\pm$ 1.37 (Table 4). These values leads to a mean SP isotopic fractionation value of -3.42 ‰ $\pm$ 1.69 and a $\delta^{15}N^{bulk}$ isotopic fractionation of -5.01 ‰ $\pm$ 1.20 (Table 4).

3.2 Pseudomonas fluorescens

Continuous measurements of the evolution of N_2O produced and consumed by the denitrifying bacteria *P. fluorescens* are presented in Fig. 6A and 6B for $\delta^{15}N^{\alpha}$ and $\delta^{15}N^{\beta}$, respectively. The correlation coefficient of the fitted Rayleigh model for the production matches the continuously measured $\delta^{15}N^{\alpha}$ data by 94.44 % on average using the R^2 method for the seven replicates of *P. fluorescens* incubations. Equivalent R^2 average for $\delta^{15}N^{\beta}$ are 94.13 %, whereas the average for $\delta^{15}N^{bulk}$ are found to be 96.86 %. The R^2 found for the reduction part is 91.92 % for $\delta^{15}N^{\alpha}$, 81.09 % for $\delta^{15}N^{\beta}$, and 92.42 % for $\delta^{15}N^{bulk}$ on average for the seven replicates. The fractionation during both the production and the reduction are therefore following the Rayleigh fractionation model to a large degree. The isotopic fractionation calculated using these models are therefore a good representation for the fractionation caused by the *P. fluorescens* bacteria on the N_2O. The resulting isotopic fractionation is presented in Table 2 for the production part and in Table 3 for the reduction part together with the calculated isotopic fractionation for the SP. During production of N_2O, the mean isotopic fractionation for SP was found to be ϵ_{SP} = 5.73 ‰ $\pm$ 5.26 while the ϵ_{bulk} = -52.21 ‰ $\pm$ 9.28 for the $\delta^{15}N^{bulk}$, hence there is a difference of 9.15 ‰ and 47.20 ‰ for ϵ_{SP} and ϵ_{bulk}, respectively, to *P. chlororaphis*. During reduction of N_2O the mean isotopic fractionation for SP was found to be ϵ_{SP} = 2.41 ‰ $\pm$ 3.04 and ϵ_{bulk} = 8.77 ‰ $\pm$ 4.49 for $\delta^{15}N^{bulk}$.

4 Discussion

The two bacteria investigated are denitrifiers, in principle functionally similar but with *P. chlororaphis* lacking the ability to reduce N_2O to N_2. Both denitrifiers were cultivated under anaerobic conditions leading to active nitric oxide reductase (both cultures) and nitrous oxide reductase (*P. fluorescens*). Fed the same amount of nitrate, we therefore expect the maximum N_2O concentration and the net N_2O production rate to be lower for *P. fluorescens* than for *P. chlororaphis*.

In Fig. 3, an example of the N_2O evolution by the two bacterial strains is plotted. The net N_2O production by *P. chlororaphis* is higher and a higher level in concentration is reached than by *P. fluorescens* even though *P. fluorescens* received six times more substrate than *P. chlororaphis*. These observations indicate that the nitrous oxide reductase consumes N_2O from a very early stage of the N_2O turnover, likely because the cultures were grown under anaerobic conditions leaving both N_2O-producing and -consuming enzymes active from the beginning of the experiment.

N_2O produced by the two denitrifying bacteria differs primarily in the bulk isotopic fractionation whereas the SP isotopic fractionation averages at a more comparable level. We find that the average difference in isotopic fractionation between *P. chlororaphis* and *P. fluorescens* is 56.58 ‰ and 10 ‰ for ϵ_{bulk} and ϵ_{SP}, respectively (Fig. 7). I.e. the isotopic fractionation is significantly higher for both isotopomers in *P. fluorescens* than in *P. chlororaphis*.

The observed difference in bulk isotopic fractionation during production of N_2O could originate from (1) a difference in the production rate, (2) a difference in the nitric oxide reductase enzymes, (3) a difference in nitrite reductase, or (4) fractionation caused by nitrous oxide reductase.

(1) The production rates in our experiments (Table 2 and 4) show a correlation between isotopic fractionation and production rate similar to the one observed by Mariotti et al. (1982). In our experiments the net production rate for *P. chlororaphis* is 10 times higher than for *P. fluorescens*, which cf. Mariotti et al. (1982) would account for only approximately a 10 ‰ offset. We therefore believe that a change in production rate does not account for the 56.58 ‰ difference in bulk isotopic fractionation alone.

(2) Nitric oxide reductase is the primary enzyme in a chain of catalytic reactions leading to the production of N_2O (Hino et al., 2010; Hendriks et al., 2000). The catalytic cycle involving production of N_2O from NO has yet to be completely understood with respect to the formation of the N-N double bond, the complexity of the structural information of nitric oxide reductase, the proton transfer pathway into nitric oxide reductase (Tosha and Shiro, 2013), and the very short lifetime of the intermediate states of the molecules (Collman et al., 2008). We hypothesized that the difference in the bulk observed during incubation of our two bacterial species was due to different nitric oxide reductases produced by the two species. To test this hypothesis, we compared the DNA sequences of the norB and norC genes coding for the large and small subunit of nitric oxide reductase, respectively, from three different strains of *P. fluorescens* (strains NCIMB 11764 [Genbank accession number CP010945], PA3G8 [742825335], and F113 [CP003150]) and *P. chlororaphis* (strains O6 [389686655], PA23 [749309655], and UFB2 [836582503]) as well as two closely related denitrifying species, *P. aeruginosa* and *P. stutzeri*. Our analysis revealed i) a very high similarity of the two genes in *P. fluorescens* and *P. chlororaphis* and ii) that the intra-species variability of the two genes was similar to the inter-species variation. This led us to reject our hypothesis and we conclude that differences in nitric oxide enzymes produced by the two species were not responsible for the observed differences in the bulk isotopic fractionation.

(3) Nitrite reductase lead to the first gaseous product during the denitrification pathway and it has been found to play an important role in isotope fractionation (Martin and Casciotti, 2016). The DNA sequences of the two bacterial strains used in our experiments revealed *P. chlororaphis* having a copper-containing nitrite reductase encoded by the gene nirK while *P. fluorescens* has a heme containing cytochrome cd1-type nitrite reductase encoded by the gene nirS. The two enzymes are structurally very different and show significantly different isotope fractionations on ϵ_{bulk} (Martin and Casciotti, 2016). Sutka and Ostrom (2006) conclude that a difference in the nitrite reductase does not have an effect on the SP during denitrification. This conclusion is based on measurements of two denitrifiers (*P. chlororaphis* (ATCC 43928) and *P. aureofaciens* (ATCC 13985)) possessing cd1-type nitrite reductase and Cu-containing nitrite reductase, respectively. We conclude the same for the two denitrifying cultures presented in this work (*P. fluorescens* and *P. chlororaphis*) since the difference in isotopic fractionation between the two bacteria species primarily is on ϵ_{bulk}.

(4) The experiments involving *P. fluorescens* are hypothesized to experience an increased fractionation during both production and reduction of N_2O as a result of simultaneous production and reduction of N_2O. After production of N_2O molecules, the light molecules degas quickly out of the liquid phase and away from the nitrous oxide reductase. The heavy N_2O molecules are slower and react with the nitrous oxide reductase leading to a depletion of the heavy N_2O isotopes. As this is a diffusion driven process it is mass-dependent and given the difference in bond energy required for breakage of the N-O bond a slight effect on SP is expected. This is also in line with the kinetic isotope effect theory which suggest a small offset towards higher

ϵ_α and therefore higher ϵ_{SP} (Popp et al., 2002; Tilsner et al., 2003; Wrage et al., 2004; Well and Flessa, 2008).

We hypothesized that the difference in ϵ_{bulk} between the two bacteria originates from 1) a difference in production rates, 3) a difference in fractionation caused by different nitrite reductases, and 4) fractionation associated with nitrous oxide reductase in *P. fluorescens*. We hypothesize that the slight difference in ϵ_{SP} originates predominantly from 4) fractionation associated with nitrous oxide reductase in *P. fluorescens*.

4.1 Comparison to previous studies

Numerous publications have presented experiments with both in situ measurements of denitrifying bacterial production and reduction of N_2O during incubation of bacterial cultures and soil samples. In Fig. 7, we present a comparison between the results from this study and the results from a selection of the previously published results. The general understanding is that denitrification results in SP $\leq$ 9 ‰. Applying different incubation techniques on soils with different properties showed SP during production of N_2O between -3 ‰ and 9 ‰ and between -0.9 ‰ and -8.2 ‰ during reduction (Well and Flessa, 2009a, b; Köster et al., 2013a; Lewicka-Szczebak et al., 2014, 2015). During production of N_2O in bacterial culture experiments involving *P. chlororaphis* (ATCC 43928), *P. aureofaciens* (ATCC 13985), and *P. denitrificans* (ATCC 17741), Thompson et al. (2004); Toyoda et al. (2005); Sutka and Ostrom (2006); Ostrom and Ostrom (2011) found ϵ_{SP} values of -27.4 ‰ and 1.3 ‰ and ϵ_{bulk} values of between -42.6 ‰ and 36.7 ‰. The wide range of ϵ_{bulk} presented both in this study and by others, confirms the difficulties in the use of ϵ_{bulk} in N_2O evolution analysis. Toyoda et al. (2005) present contrasting results for ϵ_{SP} of *P. fluorescens* (ATCC 13525) of 24.1 ‰. The result may, however, not be comparable to ours as Toyoda et al. (2005) suspect an abiological reaction within the incubation flask to be responsible for N_2O production in the incubation experiment. Our results for ϵ_{SP} calculated during N_2O production from both *P. chlororaphis* and *P. fluorescens* are in the same range as what has been reported previously.

A number of studies have investigated N_2O reduction from denitrification in soils (e.g. (Well and Flessa, 2009b; Köster et al., 2013a; Lewicka-Szczebak et al., 2014, 2015)). The results are only partly in accord with our findings for specific bacteria strains. While our results for ϵ_{bulk} are within the range of their findings, they find consistently negative ϵ_{SP} values while our results are generally positive. The only study on pure bacteria we know of is from Ostrom et al. (2007) for two bacteria strains different from ours namely *P. stutzeri* and *P. denitrificans*. They found ϵ_{SP} values between -6.8 ‰ and -5 ‰. At this point we have no explanation for the discrepancy but can find no artifact in our incubation setup.

5 Conclusions

We have presented successful continuous measurements of the denitrifying bacterial process using two different strains of bacteria: *P. fluorescens* which is a full denitrifier, and *P. chlororaphis* which is a denitrifier without nitrous oxide reductase activity. Assuming a Rayleigh type fractionation, modified for isotopomers and simultaneous reduction, we have calculated the isotopic

fractionation during production and reduction of N_2O. The isotopic fractionation for *P. chlororaphis* is in line with previous results for both SP and bulk. For *P. fluorescens*, we find similar SP isotopic fractionation values during N_2O production, while we find slightly increased SP isotopic fractionation values during N_2O reduction. The bulk isotopic fractionation calculated for N_2O reduction is in line with previously presented results though for production we find a bulk isotope depletion. We believe that, in our experiment, the bulk isotope depletion is due to a difference in production rates, in nitrite reductase, and in nitrous oxide reductase.

Author contributions. MW and TB designed the experiments and MW carried out the measurements and analyzed data. SC prepared the bacteria prior to experiments. AP analyzed the bacterial DNA sequences. DBH and EC developed the G5101i-CIC analyzer. MW prepared the manuscript with contribution from all co-authors.

Acknowledgements. We thank Jan Kaiser for isotope specific gas samples used for our reference gases, Sakae Toyoda, Naohiro Yoshida, Carina van der Veen, and Thomas Röckmann for assistance on measurements of our reference gases. We want to thank Center for Permafrost (CENPERM DNRF100) and the Centre for Ice and Climate, funded by the Danish National Research Foundation for their support, and The Danish Agency for Science Technology and Innovation, for funding used in supporting this project. We want to thank Picarro Inc. and especially Eric Crosson, and Nabil Saad for the collaboration and guidance in the development of the N_2O isotope analyzer prototype used in this project.

References

Balslev-Clausen, D. M.: Application of cavity ring down spectroscopy to isotopic bio- geo- & climate-sciences & the development of a mid-infrared CRDS analyzer for continuous measurements of N2O isotopomers, Ph.D. thesis, University of Copenhagen, 2011.

Brenninkmeijer, C. A. M. and Röckmann, T.: Mass spectrometry of the intramolecular nitrogen isotope distribution of environmental nitrous oxide using fragment-ion analysis, Rapid communications in mass spectrometry : RCM, 13, 2028–33, doi:10.1002/(SICI)1097-0231(19991030)13:20<2028::AID-RCM751>3.0.CO;2-J, 1999.

Brumback, B. a. and Rice, J. a.: Smoothing spline models for the analysis of nested and crossed sampes of curves, Journal of the American Statistical Association, 93, 961–994, 1998.

Christensen, S. and Bonde, G. J.: Seasonal variation in numbers and activity of denitrifier bacteria in soil. Taxonomy and physiological groups among isolates, Danish Journal of Plant and Soil Science, 89, 367–372, 1985.

Christensen, S. and Tiedje, J. M.: Sub-parts-per-billion nitrate method: Use of an N2O-producing denitrifier to convert NO3- or 15NO3- to N2O, Applied and environmental microbiology, 54, 1409–1413, 1988.

Ciais, P., Sabine, C., Bala, B., Bopp, L., Brovkin, V., Canadell, J., Chhabra, A., DeFries, R., Galloway, J., Heimann, M., Jones, C., Le Quéré, C., Myneni, R., Piao, S., and Thornton, P.: 6: Carbon and Other Biogeochemical Cycles, in: Carbon and Other Biogeochemical Cycles. In: Climate Change 2013: The Physical Science Basis. Contribution of Working Group I to the Fifth Assessment Report of the Intergovernmental Panel on Climate Change [Stocker, T.F., Qin, D., Plattner, G.-K., Tignor,, pp. 465–570, Cambridge University Press, Cambridge, United Kingdom and New York, NY, USA, doi:10.1017/CBO9781107415324.015, 2013.

Collman, J. P., Yang, Y., Dey, A., Decréau, R. A., Ghosh, S., Ohta, T., and Solomon, E. I.: A functional nitric oxide reductase model, Proceedings of the National Academy of Sciences of the United States of America, 105, 15 660–5, doi:10.1073/pnas.0808606105, 2008.

Denk, T., Mohn, J., Decock, C., Lewicka-Szczebak, D., Harris, E., Butterbach-Bahl, K., Kiese, R., and Wolf, B.: The nitrogen cycle: A review of isotope effects and isotope modeling approaches, Soil Biology & Biochemistry, 105, 121–137, doi:10.1016/j.soilbio.2016.11.015, 2017.

Erler, D. V., Duncan, T. M., Murray, R., Maher, D. T., Santos, I. R., Gatland, J. R., Mangion, P., and Eyre, B. D.: Applying cavity ring-down spectroscopy for the measurement of dissolved nitrous oxide concentrations and bulk nitrogen isotopic composition in aquatic systems : Correcting for interferences and field application, Limnology and Oceanography, 13, 391–401, doi:10.1002/lom3.10032, 2015.

Firestone, M. K. and Davidson, E. A.: Microbiological basis of NO and N2O production and consumption in soil, Exchange of Trace Gases between Terrestrial Ecosystems and the Atmosphere, pp. 7–21, 1989.

Forster, P., Ramaswamy, V., Artaxo, P., Berntsen, T., Betts, R., Fahey, D., Lean, J. H. J., Lowe, D., Myhre, G., Prinn, J. N. R., Raga, G., Schulz, M., and Dorland, R. V.: Climate Change 2007: The Physical Science Basis. Contribution of Working Group I to the Fourth Assessment Report of the Intergovernmental Panel on Climate Change, chapter Changes in Atmospheric Constituents and in Radiative Forcing, Cambridge University Press, Cambridge, United Kingdom and New York, NY, USA., pp. 130–217, 2007.

Hartmann, D., Klein Tank, A., Rusticucci, M., Alexander, L., Brönnimann, S., Charabi, Y., Dentener, F., Dlugokencky, E., Easterling, D., Kaplan, A., Soden, B., Thorne, P., Wild, M., and Zhai, P.: 2013: Observations: Atmosphere and Surface. In: Climate Change 2013: The Physical Science Basis. Contribution of Working Group I to the Fifth Assessment Report of the Intergovernmental Panel on Climate Change, Cambridge University Press, Cambridge, United Kingdom and New York, NY, USA, 2013.

Heil, J., Wolf, B., Brüggemann, N., Emmenegger, L., Tuzson, B., Vereecken, H., and Mohn, J.: Site-specific 15N isotopic signatures of abiotically produced N2O, Geochimica et Cosmochimica Acta, 139, 72–82, doi:10.1016/j.gca.2014.04.037, 2014.

Hendriks, J., Oubrie, A., Castresana, J., Urbani, A., Gemeinhardt, S., and Saraste, M.: Nitric oxide reductases in bacteria, Biochimica et biophysica acta, 1459, 266–273, doi:10.1016/S0005-2728(00)00161-4, 2000.

Hino, T., Matsumoto, Y., Nagano, S., Sugimoto, H., Fukumori, Y., Murata, T., Iwata, S., and Shiro, Y.: Structural Basis of Biological N2O Generation by Bacterial Nitric Oxide Reductase, Science, 330, 1666–1670, doi:10.1126/science.1195591, 2010.

Kaiser, J.: Stable isotope investigations of atmospheric nitrous oxide, Ph.D. thesis, Johannes Gutenberg-Universität Mainz, 2002.

Kim, K. R. and Craig, H.: Nitrogen-15 and oxygen-18 characteristics of nitrous oxide: A global perspective, Science, 262, 1993.

Köster, J. R., Well, R., Dittert, K., Giesemann, A., Lewicka-Szczebak, D., Mühling, K. H., Herrmann, A., Lammel, J., and Senbayram, M.: Soil denitrification potential and its influence on N2O reduction and N2O isotopomer ratios, Rapid Communications in Mass Spectrometry, 27, 2363–2373, doi:10.1002/rcm.6699, 2013a.

Köster, J. R., Well, R., Tuzson, B., Bol, R., Dittert, K., Giesemann, A., Emmenegger, L., Manninen, A., Cárdenas, L., and Mohn, J.: Novel laser spectroscopic technique for continuous analysis of N2O isotopomers - Application and intercomparison with isotope ratio mass spectrometry, Rapid Communications in Mass Spectrometry, 27, 216–222, doi:10.1002/rcm.6434, 2013b.

Lewicka-Szczebak, D., Well, R., Köster, J. R., Fuß, R., Senbayram, M., Dittert, K., and Flessa, H.: Experimental determinations of isotopic fractionation factors associated with N2O production and reduction during denitrification in soils, Geochimica et Cosmochimica Acta, 134, 55–73, doi:10.1016/j.gca.2014.03.010, 2014.

Lewicka-Szczebak, D., Well, R., Bol, R., Gregory, A., Matthews, G., Misselbrook, T., Whalley, W., and Cardenas, L.: Isotope fractionation factors controlling isotopocule signatures of soil-emitted N2O produced by denitrification processes of various rates, Rapid Communications in Mass Spectrometry, 29, 269–282, doi:10.1002/rcm.7102, 2015.

Lord Rayleigh, S. R.: Theoretical considerations respecting the separation of gases by diffusion and similar processes, Philosophical Magazine Series 5, 42, 493–498, doi:10.1080/14786449608620944, http://dx.doi.org/10.1080/14786449608620944, 1896.

Mariotti, A., Germon, J. C., Hubert, P., Kaiser, P., Letolle, R., Tardieux, A., and Tardieux, P.: Experimental determination of nitrogen kinetic isotope fractionation: some principles; illustration for the denitrification and nitrification processes, Plant and soil, 430, 413–430, 1981.

Mariotti, A., Germon, J. C., and Leclerc, A.: Nitrogen isotope fractionation associated with the NO2- to N2O step of denitrification in soils, Canadian journal of soil science, 62, 227–241, 1982.

Martin, T. S. and Casciotti, K. L.: Nitrogen and oxygen isotopic fractionation during microbial nitrite reduction, Limnology and Oceanography, 61, 1134–1143, doi:10.1002/lno.10278, 2016.

Menyailo, O. V. and Hungate, B. A.: Stable isotope discrimination during soil denitrification: Production and consumption of nitrous oxide, Global Biogeochemical Cycles, 20, n/a–n/a, doi:10.1029/2005GB002527, 2006.

Mohn, J., Guggenheim, C., Tuzson, B., Vollmer, M. K., Toyoda, S., Yoshida, N., and Emmenegger, L.: A liquid nitrogen-free preconcentration unit for measurements of ambient N2O isotopomers by QCLAS, Atmospheric Measurement Techniques, 3, 609–618, doi:10.5194/amt-3-609-2010, 2010.

Mohn, J., Tuzson, B., Manninen, A., Yoshida, N., Toyoda, S., Brand, W. a., and Emmenegger, L.: Site selective real-time measurements of atmospheric N2O isotopomers by laser spectroscopy, Atmospheric Measurement Techniques, 5, 1601–1609, doi:10.5194/amt-5-1601-2012, http://www.atmos-meas-tech.net/5/1601/2012/, 2012.

Mohn, J., Wolf, B., Toyoda, S., Lin, C. T., Liang, M. C., Brüggemann, N., Wissel, H., Steiker, A. E., Dyckmans, J., Szwec, L., Ostrom, N. E., Casciotti, K. L., Forbes, M., Giesemann, A., Well, R., Doucett, R. R., Yarnes, C. T., Ridley, A. R., Kaiser, J., and Yoshida, N.: Interlaboratory assessment of nitrous oxide isotopomer analysis by isotope ratio mass spectrometry and laser spectroscopy: Current status and perspectives, Rapid Communications in Mass Spectrometry, 28, 1995–2007, doi:10.1002/rcm.6982, 2014.

Mosier, A., Kroeze, C., and Nevison, C.: Closing the global N2O budget: nitrous oxide emissions through the agricultural nitrogen cycle, Nutrient Cycling in Agroecosystems, 52, 225–248, 1998.

Olivier, J. G. J., Bouwman, A. F., Van der Hoek, K. W., and Berdowski, J. J. M.: Global air emission inventories for anthropogenic sources of NOx, NH3, and N2O in 1990, Environmental Pollution, 102, 135–148, 1998.

Ostrom, N. E. and Ostrom, P. H.: The isotopomers of Nitrous oxide: Analytical considerations and application to resolution of microbial production pathways, in: Handbook of Environmental Isotope Geochemistry, edited by Baskaran, M., pp. 453–476, Springer Berlin Heidelberg, Berlin, Heidelberg, doi:10.1007/978-3-642-10637-8, http://link.springer.com/10.1007/978-3-642-10637-8, 2011.

Ostrom, N. E., Pitt, A., Sutka, R., Ostrom, P. H., Grandy, A. S., Huizinga, K. M., and Robertson, G. P.: Isotopologue effects during N2O reduction in soils and in pure cultures of denitrifiers, Journal of Geophysical Research, 112, G02 005, doi:10.1029/2006JG000287, 2007.

Park, S., Pérez, T., Boering, K. A., Trumbore, S. E., Gil, J., Marquina, S., and Tyler, S. C.: Can N2O stable isotopes and isotopomers be useful tools to characterize sources and microbial pathways of N2O production and consumption in tropical soils?, Global Biogeochemical Cycles, 25, GB1001, doi:10.1029/2009GB003615, 2011.

Pérez, T., Trumbore, S. C., Tyler, S. C., Davidson, E. A., Keller, M., and De Camargo, P. B.: Isotopic variability of N2O emissions from tropical forest soils, Global Biogeochemical Cycles, 14, 525–535, 2000.

Pérez, T., Trumbore, S. E., Tyler, S. C., Matson, P. A., Ortiz-Monasterio, I., Rahn, T., and Griffith, D. W. T.: Identifying the agricultural imprint on the global N2O budget using stable isotopes, Journal of Geophysical Research, 106, 9869–9878, doi:10.1029/2000JD900809, 2001.

Popp, B. N., Westley, M. B., Toyoda, S., Miwa, T., Dore, J. E., Yoshida, N., Rust, T. M., Sansone, F. J., Russ, M. E., Ostrom, N. E., and Ostrom, P. H.: Nitrogen and oxygen isotopomeric constraints on the origins and sea-to-air flux of N2O in the oligotrophic subtropical North Pacific gyre, Global Biogeochemical Cycles, 16, 12–1–12–10, doi:10.1029/2001GB001806, http://doi.wiley.com/10.1029/2001GB001806, 2002.

Schilt, A., Baumgartner, M., Schwander, J., Buiron, D., Capron, E., Chappellaz, J., Loulergue, L., Schüpbach, S., Spahni, R., Fischer, H., and Stocker, T. F.: Atmospheric nitrous oxide during the last 140.000years, Earth and Planetary Science Letters, 300, 33–43, doi:10.1016/j.epsl.2010.09.027, 2010.

Stuart Chapin III, F., Matson, P. A., and Mooney, H. A.: Principles of terrestrial ecosystem ecology, Springer-Verlag, New York, 2002.

Sutka, R. L. and Ostrom, N. E.: Distinguishing nitrous oxide production from nitrification and denitrification on the basis of isotopomer abundances, Applied and environmental microbiology, 72, 638–644, doi:10.1128/AEM.72.1.638, 2006.

Thompson, A. E., Park, S., Firestone, M., Amundson, R., and Boering, K.: Variable Nitrogen Isotope Effects Associated With N2O Isotopologue Production: Towards an Understanding of Denitrification Mechanism, AGU Fall Meeting Abstracts, http://adsabs.harvard.edu/abs/2004AGUFM.B11C..03T, 2004.

Tilsner, J., Wrage, N., Lauf, J., and Gebauer, G.: Emission of gaseous nitrogen oxides from an extensively managed grassland in NE Bavaria, Germany. II. Stable isotope natural abundance of N2O, Biogeochemistry, 63, 249–267, doi:10.1023/A:1023316315550, 2003.

Tosha, T. and Shiro, Y.: Crystal structures of nitric oxide reductases provide key insights into functional conversion of respiratory enzymes, IUBMB Life, 65, 217–226, doi:10.1002/iub.1135, 2013.

Toyoda, S., Yoshida, N., Miwa, T., Matsui, Y., Yamagishi, H., and Tsunogai, U.: Production mechanism and global budget of N2O inferred from its isotopomers in the western North Pacific, Geophysical Research Letters, 29, 5–8, 2002.

Toyoda, S., Mutobe, H., Yamagishi, H., Yoshida, N., and Tanji, Y.: Fractionation of N2O isotopomers during production by denitrifier, Soil Biology and Biochemistry, 37, 1535–1545, doi:10.1016/j.soilbio.2005.01.009, http://linkinghub.elsevier.com/retrieve/pii/S0038071705000404, 2005.

Waechter, H., Mohn, J., Tuzson, B., Emmenegger, L., and Sigrist, M. W.: Determination of N2O isotopomers with quantum cascade laser based absorption spectroscopy, Optics express, 16, 9239–9244, doi:10.1364/OE.16.00923, 2008.

Well, R. and Flessa, H.: Isotope fractionation factors of N2O diffusion, Rapid Communications in Mass Spectrometry, 22, 2621–2628, doi:10.1002/rcm, 2008.

Well, R. and Flessa, H.: Isotopologue signatures of N2O produced by denitrification in soils, Journal of Geophysical Research, 114, G02 020, doi:10.1029/2008JG000804, 2009a.

Well, R. and Flessa, H.: Isotopologue enrichment factors of N2O reduction in soils, Rapid Communications in Mass Spectrometry, pp. 2996–3002, doi:10.1002/rcm, 2009b.

Wrage, N., Velthof, G. L., Beusichem, M. L. V., and Oenema, O.: Role of nitrifier er denitrication in the production of nitrous oxide, Soil Biology and Biochemistry, 33, 1723–1732, 2001.

Wrage, N., Lauf, J., del Prado, a., Pinto, M., Pietrzak, S., Yamulki, S., Oenema, O., and Gebauer, G.: Distinguishing sources of N2O in European grasslands by stable isotope analysis, Rapid Communications in Mass Spectrometry, 18, 1201–1207, doi:10.1002/rcm.1461, http://www.ncbi.nlm.nih.gov/pubmed/15164349, 2004.

Yoshida, N. and Toyoda, S.: Constraining the atmospheric N2O budget from intramolecular site preference in N2O isotopomers, Nature, 405, 330–4, doi:10.1038/35012558, 2000.

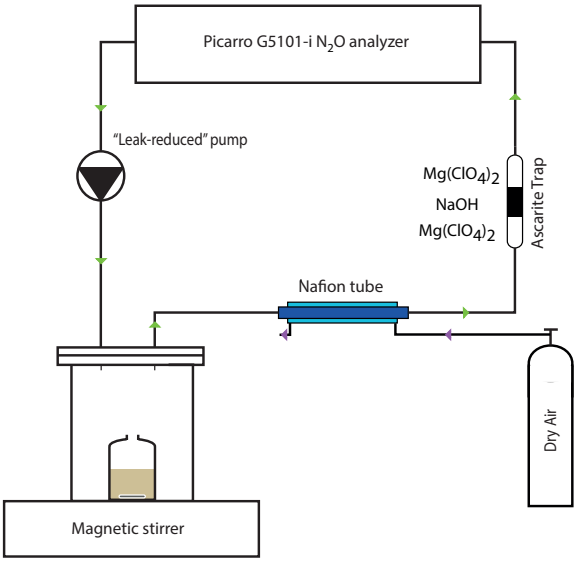

Figure 1. Simplified schematic of the incubation setup. The green and the purple arrows show the flow direction of the measuring gas and the purge gas, respectively.

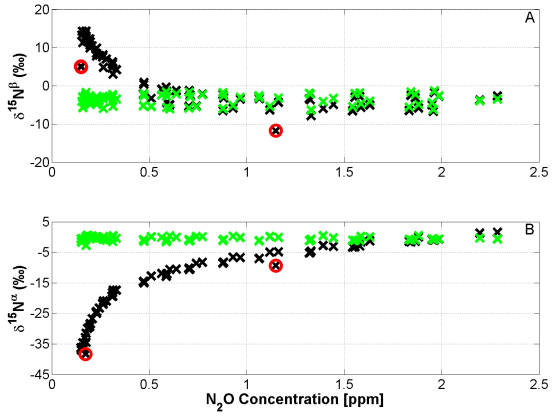

Figure 2. The concentration-dependent correction (CDC) for (A) $\delta^{15}N^{\alpha}$ and (B) $\delta^{15}N^{\beta}$ respectively. In both Figures, the raw data are presented in black, the CDC data is plotted in green, and the outliers are marked with red circles.

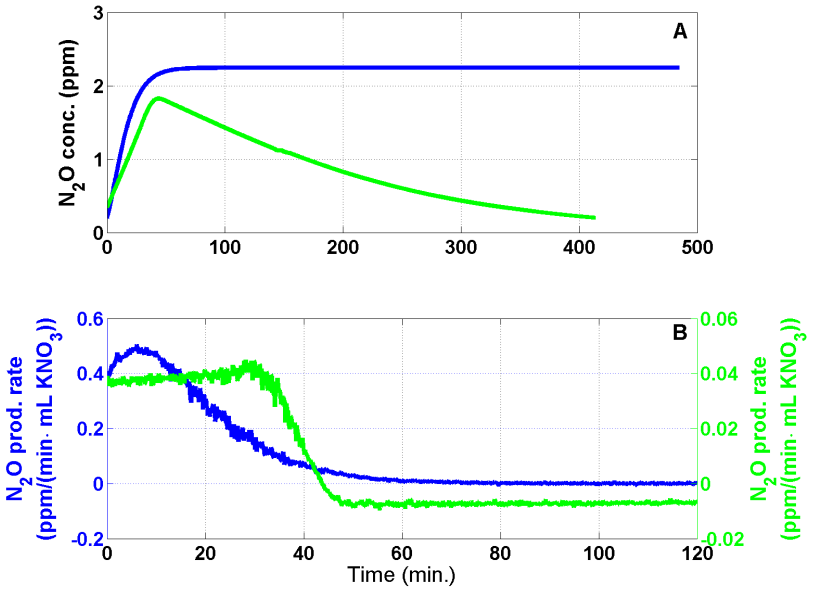

Figure 3. Continuous measurements of (A) N_2O concentrations and (B) the net N_2O production rate from experiments with *P. fluorescens* (green) and *P. chlororaphis* (blue), respectively. Only the first 120 minutes of the net N_2O production are shown. Note that the scaling of the two horizontal axis differs.

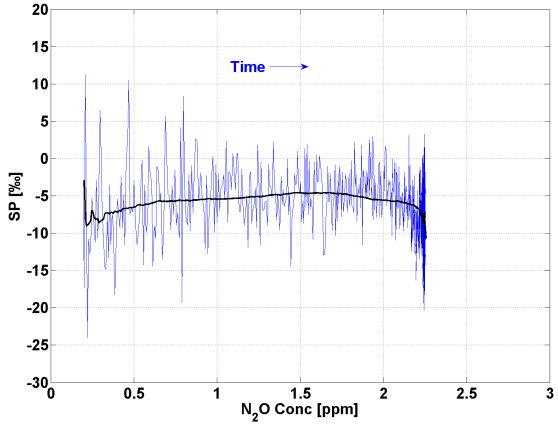

Figure 4A. SP as a function of N_2O concentration as produced by *P. chlororaphis*. High resolution CRDS data (blue line) and five minutes running average (black line). The blue arrow indicates the direction of time during production of N_2O.

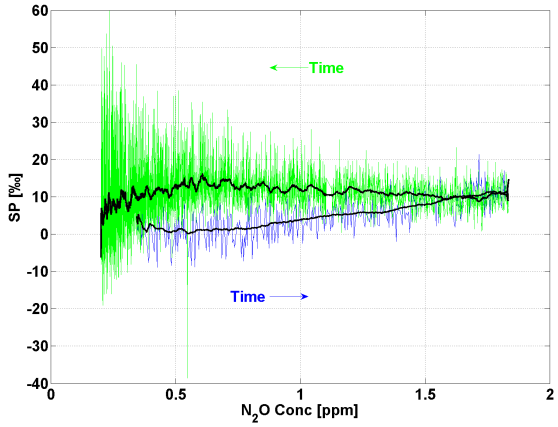

Figure 4B. SP as a function of N_2O concentration produced by *P. fluorescens*. High resolution CRDS data (blue and green line) and five minutes running average (black line). The blue arrow indicates the direction of time during production of N_2O whereas the green arrow indicates the direction of time during reduction of N_2O.

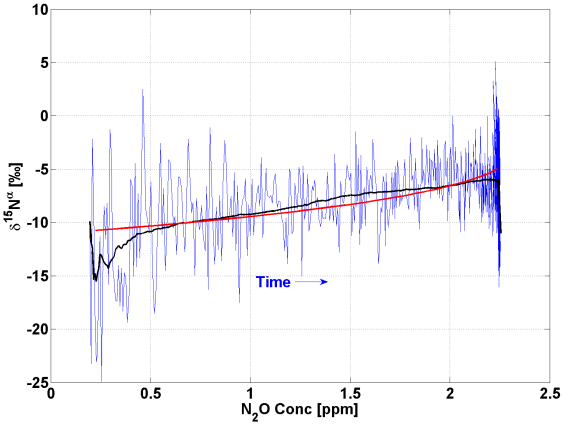

Figure 5A. $\delta^{15}N^{\alpha}$ as a function of N_2O concentration as produced by *P. chlororaphis* and the modeled Rayleigh type distillation. High resolution CRDS data (blue line) and five minutes running average (black line). The red curve is the modeled Rayleigh type distillation curve for the production of N_2O. The blue arrow indicates the direction of time during production of N_2O.

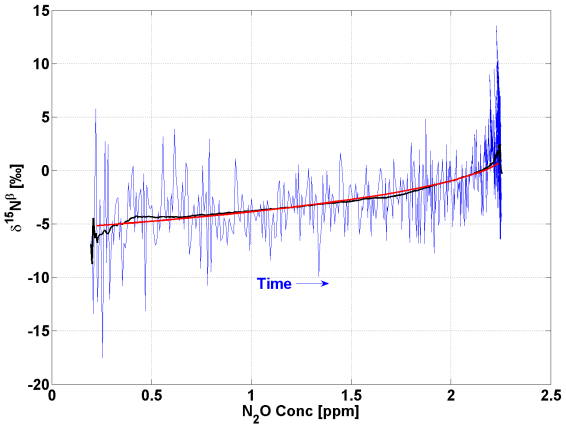

Figure 5B. $\delta^{15}N^{\beta}$ as a function of N_2O concentration as produced by *P. chlororaphis* and the modeled Rayleigh type distillation. High resolution CRDS data (blue line) and five minutes running average (black line). The red curve is the modeled Rayleigh type distillation curve for the production of N_2O. The blue arrow indicates the direction of time during production of N_2O.

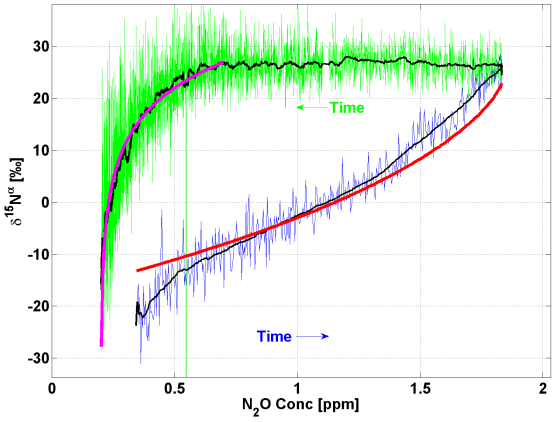

Figure 6A. $\delta^{15}N^{\alpha}$ as a function of N_2O concentration produced by *P. fluorescens* with the modeled Rayleigh type distillation. High resolution CRDS data (blue and green line) and five minutes running average (black line). The red and magenta curves are the modeled Rayleigh type distillation curves for the production and reduction of N_2O, respectively. The blue arrow indicates the direction of time during production of N_2O whereas the green arrow indicates the direction of time during reduction of N_2O.

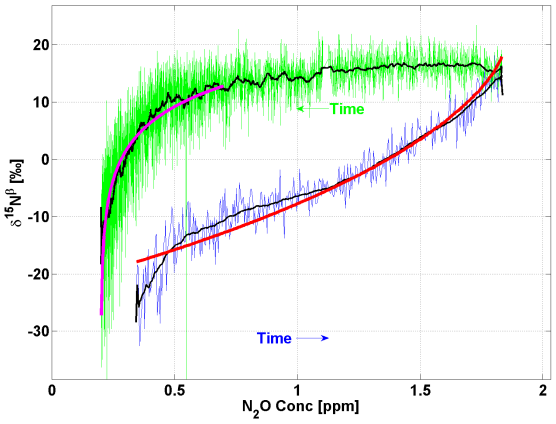

Figure 6B. $\delta^{15}N^{\beta}$ as a function of N_2O concentration produced by *P. fluorescens* with the modeled Rayleigh type distillation. High resolution CRDS data (blue and green line) and five minutes running average (black line). The red and magenta curves are the modeled Rayleigh type distillation curves for the production and reduction of N_2O, respectively. The blue arrow indicates the direction of time during production of N_2O whereas the green arrow indicates the direction of time during reduction of N_2O.

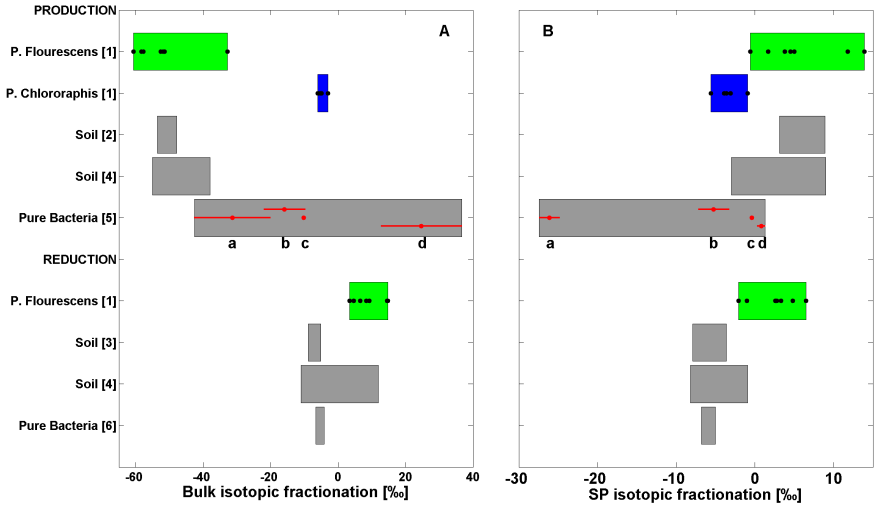

Figure 7. (A) Bulk and (B) SP isotopic fractionation calculated from the continuous measurements with *P. fluorescens* (green) and *P. chlororaphis* (blue) respectively. Both the production and reduction isotopic fractionations are shown and compared with previously presented results. [1] [This study], [2] [Well and Flessa (2009a)], [3] [Well and Flessa (2009b)], [4] [Lewicka-Szczebak et al. (2014, 2015)], [5] [a) Thompson et al. (2004), b) Toyoda et al. (2005), c) Ostrom and Ostrom (2011) d) Sutka and Ostrom (2006)], [6] [Ostrom et al. (2007)].

Table 1. Measurements of standard gas CIC-MPI-1 and CIC-MPI-2, diluted MPI-1 and MPI-2 gases respectively. Measurements were measured at the four respective institutes. The combined mean-values (Cmean) and standard deviations are calculated from measurements performed at Tokyo-Tech, IMAU, and CIC. The root-mean-square deviations (RMSD) are calculated against the original UEA data.

Std. gas	Institute	$[N_2O]$ (ppb)	$\delta^{15}N^{bulk}$ (‰)	$\delta^{15}N^{\alpha}$ (‰)	$\delta^{15}N^{\beta}$ (‰)
MPI-1	UEA	-	1.00 ± 0.03	0.70 ± 0.90	1.30 ± 0.90
CIC-MPI-1					
	Tokyo-Tech	1828.9 ± 4.9	1.34 ± 0.17	1.44 ± 0.09	1.24 ± 0.35
	IMAU	1919.3 ± 21.0	1.08 ± 0.10	2.31 ± 0.25	-0.15 ± 0.33
	CIC	1918.4 ± 2.3	2.62 ± 1.77	0.29 ± 2.44	4.95 ± 2.37
	Cmean	1909.8 ± 29.3	1.32 ± 0.82	1.94 ± 0.87	0.70 ± 1.42
	RMSD	-	0.96	1.05	2.27
MPI-2	UEA		-1.78 ± 0.03	12.40 ± 0.04	-15.90 ± 0.90
CIC-MPI-2					
	Tokyo-Tech	1840.2 ± 32.1	-1.30 ± 0.06	12.79 ± 0.22	-15.41 ± 0.24
	IMAU	1865.9 ± 16.0	-1.68 ± 0.10	11.80 ± 0.37	-15.16 ± 0.46
	CIC	1827.2 ± 1.8	-0.15 ± 1.78	12.58 ± 2.51	-12.89 ± 2.35
	Cmean	1857.9 ± 19.2	-1.43 ± 0.82	12.01 ± 1.06	-14.87 ± 1.13
	RMSD	-	0.98	0.43	1.81

Table 2. Isotopic fractionation, reduction correction parameter (γ), extremes of the unreacted fraction parameter (f_{start} and f_{end}), and production rate (k_p) in $[\mathrm{ppm}/(\mathrm{min} \cdot \mathrm{mL\ KNO_3})]$ for the production of N_2O from *P. fluorescens*.

Replica #	ϵ_{α} (‰)	ϵ_{β} (‰)	ϵ_{bulk}(‰)	ϵ_{SP} (‰)	γ	f_{start}	f_{end}	k_p
1	-55.50	-60.00	-57.75	4.50	0.00	0.38	0.000	0.035
2	-33.10	-32.50	-32.80	-0.60	0.52	0.94	0.000	0.078
3	-49.40	-54.40	-51.90	5.00	0.19	0.42	0.000	0.031
4	-59.80	-61.50	-60.65	1.70	0.00	0.68	0.000	0.016
5	-46.70	-58.50	-52.60	11.80	0.35	0.94	0.003	0.006
6	-56.40	-60.20	-58.30	3.80	0.04	0.69	0.007	0.005
7	-44.50	-58.40	-51.45	13.90	0.14	0.68	0.008	0.012
Mean	**-49.34 ± 9.05**	**-55.07 ± 10.20**	**-52.21 ± 9.28**	**5.73 ± 5.26**	**0.18 ± 0.20**	**0.68 ± 0.22**	**0.003 ± 0.004**	**0.026 ± 0.026**

Table 3. Isotopic fractionation, extremes of the unreacted fraction parameter (f_{start} and f_{end}), and reduction rate (k_r) in $[\mathrm{ppm}/(\mathrm{min} \cdot \mathrm{mL\ KNO_3})]$ for the reduction of N_2O from *P. fluorescens*.

Replica #	ϵ_α (‰)	ϵ_β (‰)	ϵ_{bulk}(‰)	ϵ_{SP} (‰)	f_{start}	f_{end}	k_r
1	9.70	7.10	8.30	2.60	1	0	-0.0027
2	3.10	4.10	3.40	-1.00	1	0	-0.0060
3	11.00	7.70	9.30	3.30	1	0	-0.0022
4	3.70	5.80	4.60	-2.10	1	0	-0.0027
5	18.20	11.70	14.80	6.50	1	0	-0.0014
6	17.10	12.30	14.50	4.80	1	0	-0.0019
7	9.30	6.50	6.50	2.80	1	0	-0.0009
Mean	**10.30 ± 5.86**	**7.89 ± 3.04**	**8.77 ± 4.49**	**2.41 ± 3.04**	**1 ± 0**	**0 ± 0**	**-0.003 ± 1.7e^{-3}**

Table 4. Isotopic fractionation, extremes of the unreacted fraction parameter (f_{start} and f_{end}), and production rate (k_p) in $[\mathrm{ppm}/(\mathrm{min} \cdot \mathrm{mL\ KNO_3})]$ for the production of N_2O from *P. chlororaphis*.

Replica #	ϵ_α (‰)	ϵ_β (‰)	ϵ_{bulk}(‰)	ϵ_{SP} (‰)	f_{start}	f_{end}	k_p
1	-8.70	-3.10	-5.90	-5.60	1	0	0.237
2	-5.00	-1.10	-3.05	-3.90	1	0	0.250
3	-6.90	-3.30	-5.10	-3.60	1	0	0.215
4	-5.40	-4.40	-4.95	-0.90	1	0	0.182
5	-7.60	-4.50	-6.05	-3.10	1	0	0.126
Mean	**-6.72 ± 1.54**	**-3.28 ± 1.37**	**-5.01 ± 1.20**	**-3.42 ± 1.69**	**1 ± 0**	**0 ± 0**	**0.201 ± 0.049**

1 Supporting material

1.1 Oxygen dependence

The gas matrix of the sample gas is of great importance when using spectroscopy based measuring techniques. When the mixing ratio of the gas matrix is changed, the line shape is also altered, leading to a change in the isotopic signature of the measured sample gas. For the CRDS analyzers, the isotopic signature of the N_2O isotopologues has a linear response to the oxygen availability in the gas matrix (Erler et al., 2015).

The presented bacterial experiments are performed under anaerobic conditions, where oxygen (O_2) is not present. The effect of this lack of O_2 on the isotopic signal was quantified by performing dilution experiments on the two CIC-MPI standard gasses. Two stepwise dilution measurement with either pure synthetic air or N_2 was conducted for each of the standard gases. The N_2 was of purity 99.9999 % and the synthetic air was a N_2/O_2 mixture (20.1 % O_2 and 79.9 % N_2, purity 99.999 %). Figure S1 show the average measured $\delta^{15}N^{\alpha}$ values for each step during each of the four four dilution experiments. Similar measurements were performed on $\delta^{15}N^{\beta}$ and $\delta^{15}N^{bulk}$. The two dilution experiments with synthetic air (Fig. S1A and S1B) results in a dependence only on the N_2O concentration. The two dilution experiments with N_2 (Fig. S1C and S1D) results in a dependence on both the N_2O concentration and the O_2 concentration.

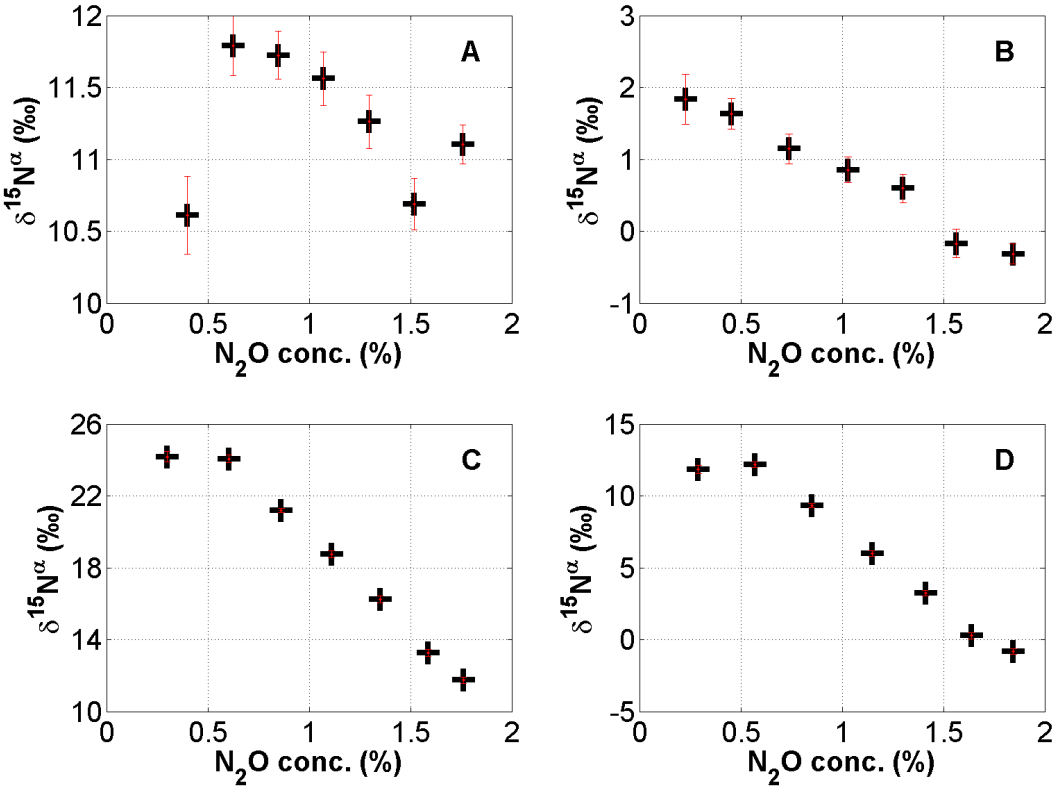

Figure S1. *The results of the four dilution experiments for $\delta^{15}N^{\alpha}$. (A) CIC-MPI-II diluted with synthetic air (B) CIC-MPI-I diluted with synthetic air, (C) CIC-MPI-II diluted with N_2, and (D) CIC-MPI-I diluted with N_2. Black points represent the mean of 30 minutes continuous measurements. The standard error (error bars) of the measurements are shown in red.*

The effect of a changing O_2 concentration on the isotopic composition of N_2O is assessed from the difference between the two dilution experiments for each standard gas. When calculating the difference between the two dilution experiments we isolate the dependence on the O_2 concentration, i.e. the difference in $\delta^{15}N^{\alpha}$ is plotted versus the O_2 concentration. Figure S2 show the difference between dilution experiments performed with synthetic air and N_2. I.e. the difference between Fig. S1A and Fig. S1C for CIC-MPI-II and the difference between Fig. S1B and Fig. S1D for CIC-MPI-I. Similar measurements were performed on $\delta^{15}N^{\beta}$ and $\delta^{15}N^{bulk}$.

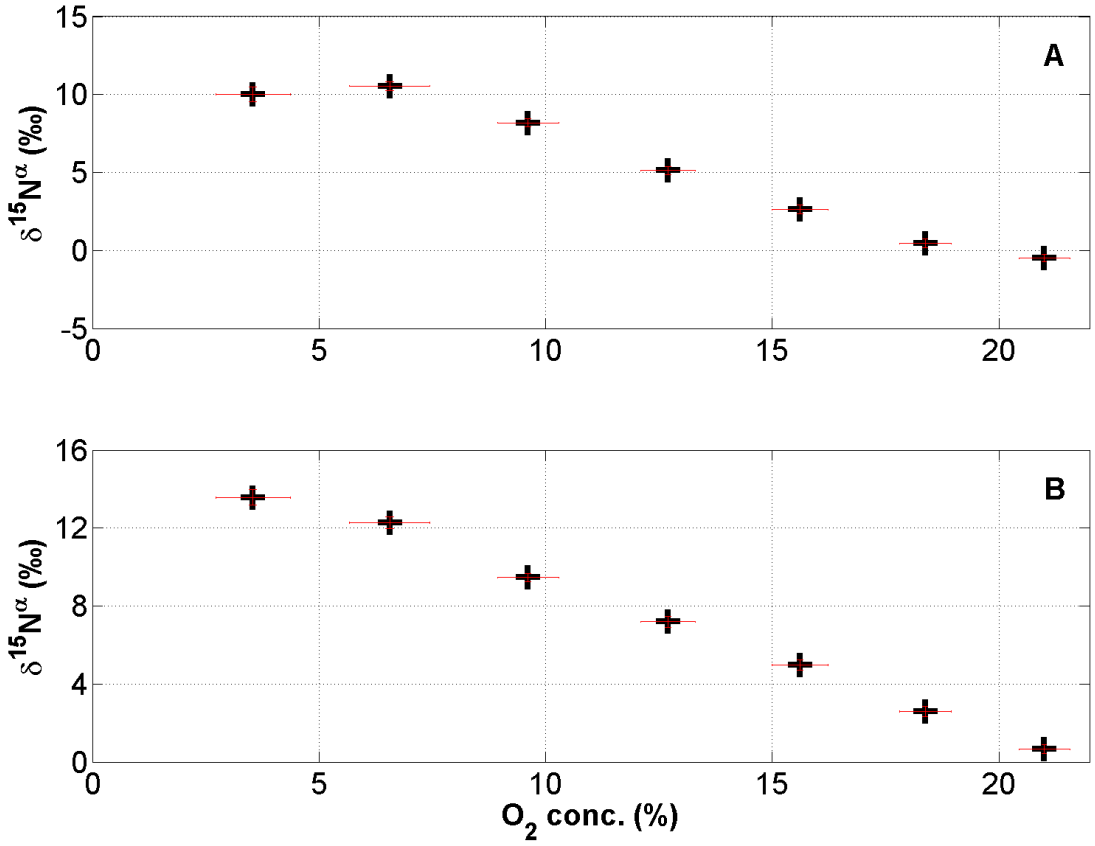

Figure S2. *The results of the difference between dilution experiments performed with synthetic air and N_2 performed on $\delta^{15}N^{\alpha}$. (A) difference measured on CIC-MPI-I, and (B) difference measured on CIC-MPI-II. Black points represent the mean of 30 minutes continuous measurements. The standard error (error bars) of the measurements are shown in red for both the δ-value and the O_2 concentration.*

The average response of the isotope composition with respect to the O_2 concentration averaged for the two standard gasses are presented in Fig. S3. This relation is calculated using a Monte Carlo algorithm applied to a linear relation model for the O_2 concentration and $\delta^{15}N^{\alpha}$, $\delta^{15}N^{\beta}$, and $\delta^{15}N$ respectively.

The linear relation model for the effect of O_2 concentration ($[O_2]$) to the values of $\delta^{15}N^{\alpha}$, $\delta^{15}N^{\beta}$, and $\delta^{15}N$ are shown in equation 1, 2, and 3, respectively.

$$\delta^{15}N^{\alpha}_{ODC} = -0.1534 \cdot [O_2] + 15.27 \quad (1)$$

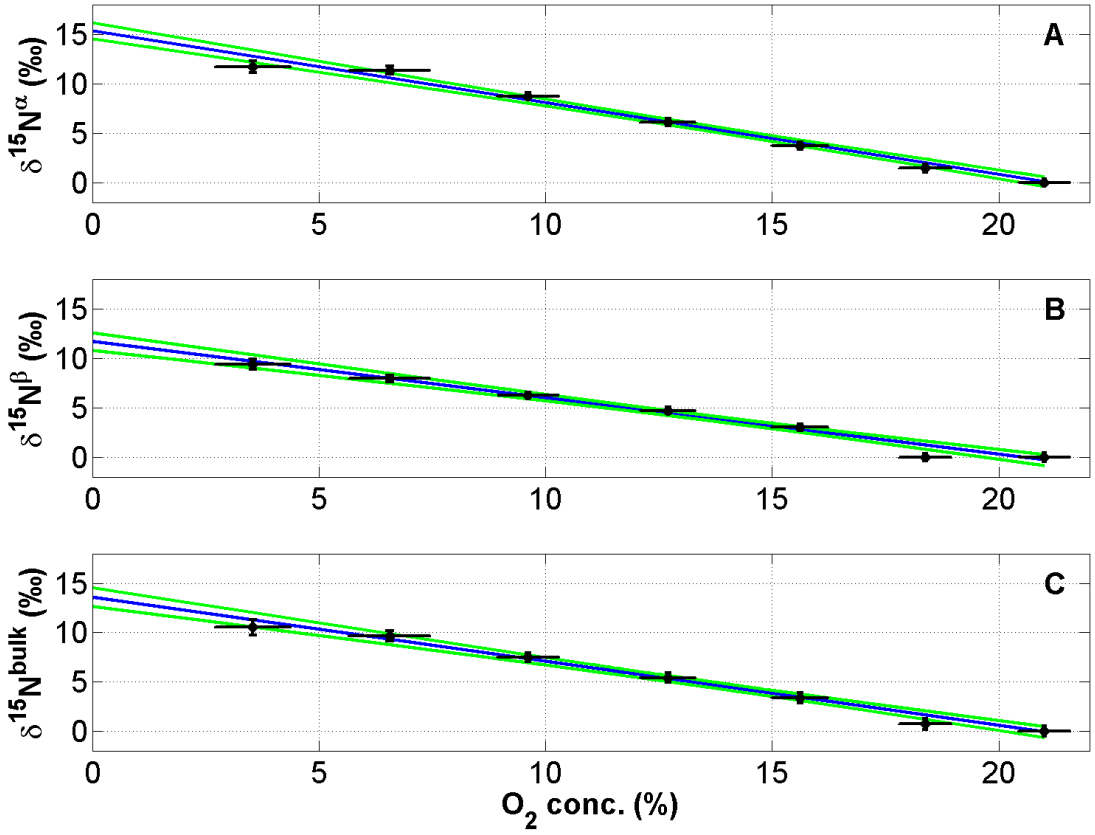

Figure S3. *The effect of changing O_2 concentration on the (A) $\delta^{15}N^{\alpha}$, (B) $\delta^{15}N^{\beta}$, and (C) $\delta^{15}N$. Black points represent the response of the isotope composition with respect to the O_2 concentration averaged for the two standard gasses. The standard error (error bars) of the measurements are shown in black for both the δ-value and the O_2 concentration. The blue lines are mean values of the Monte Carlo simulation. The green lines are the 1-σ error-bar calculated using Monte Carlo simulation.*

$$\delta^{15}N^{\beta}_{ODC} = -0.1210 \cdot [O_2] + 11.66 \tag{2}$$

$$\delta^{15}N^{bulk}_{ODC} = -0.1372 \cdot [O_2] + 13.47 \tag{3}$$

In the above $\delta^{15}N^{\alpha}_{ODC}$, $\delta^{15}N^{\beta}_{ODC}$, and $\delta^{15}N^{bulk}_{ODC}$ represent the offsets which are subtracted from the N_2O concentration corrected data.

The bacterial evolution experiments were performed under pure N_2 conditions. The reported values in the article, are derived by first applying the N_2O concentration correction and then subsequently applying the correction for the lack of O_2. With zero O_2 this correction becomes a simple subtraction by the intercept values of the above linear models.

1.2 Rayleigh model for isotopomers of N_2O

Mariotti et al. (1981) derived the equation for the isotope ratio of the substrate as:

$$\frac{R_s}{R_{s,0}} = f^{(\alpha_{p/s}-1)} \tag{4}$$

where $R_{s,0}$ is the initial isotope ratio of the substrate, R_s is the isotope ratio of the substrate at time t, $\alpha_{p/s}$ is the fractionation factor of the product versus the substrate, and f is the unreacted fraction of substrate at time t. I.e. f is going in steps from 1 to 0 during the reaction. The fractionation factor of the product versus the substrate is the bulk fractionation factor α_{bulk}, and therefore $\alpha_{bulk} = (\alpha_\alpha + \alpha_\beta)/2$.

The fractionation factor is a constant calculated as $\alpha_{p/s} = R_p/R_s$. The immediate product for the two isotopomers (R^i_{im}) therefore calculates as:

$$R^i_{im} = R_s \cdot \alpha_i \tag{5}$$

$$\Updownarrow$$

$$R^i_{im} = \alpha_i \cdot R_{s,0} \cdot f^{(\alpha_{bulk}-1)} \tag{6}$$

where the isotopomers are distinguished with i ($i = 1, 2$), respectively. The accumulated product for each of the isotopomers ($R^i_{p,acc}$) can therefore be calculated as the sum of the respective immediate products.

$$R^i_{p,acc} = \frac{1}{1-f}\int_f^1 R^i_{im} df' \tag{7}$$

$$\Updownarrow$$

$$R^i_{p,acc} = \frac{1}{1-f}\int_f^1 \alpha_i \cdot R_{s,0} \cdot f'^{(\alpha_{bulk}-1)} df'. \tag{8}$$

where f is the unreacted fraction of the substrate. The equation for the accumulated product for each of the isotopomers derives to:

$$R^i_{p,acc} = \alpha_i \cdot \frac{R_{s,0}}{1-f}\int_f^1 f'^{(\alpha_{bulk}-1)} df \tag{9}$$

$$\Downarrow$$

$$R^i_{p,acc} = \alpha_i \cdot \frac{R_{s,0}}{1-f} \cdot \left[\frac{f'^{\alpha_{bulk}}}{\alpha_{bulk}}\right]_f^1 \tag{10}$$

$$\Downarrow$$

$$R^i_{p,acc} = \frac{\alpha_i}{\alpha_{bulk}} \cdot R_{s,0} \cdot \frac{1-f^{\alpha_{bulk}}}{1-f} \tag{11}$$

$$\Downarrow$$

$$R^i_{p,acc} = \frac{\alpha_i}{\alpha_{bulk}} \cdot R^{bulk}_{p,acc}. \tag{12}$$

The isotopomer correction factors for the two isotopomers (φ_α and φ_β) therefore ends up as presented in the manuscript.

$$\varphi_\alpha = \frac{\alpha_\alpha}{\alpha_{bulk}} \quad , \quad \varphi_\beta = \frac{\alpha_\beta}{\alpha_{bulk}} \tag{13}$$

1.3 Iterative determination of unreacted fraction (f)

1.3.1 Figures of f_{start} for $\delta^{15}N^{\alpha}$

Figures of the iterative determination of the starting point of the unreacted fraction (f) of $\delta^{15}N^{\alpha}$ versus the calculated R-squared value. The black crosses are all possible f-values used in calculation of R^2 between the Rayleigh fractionation profile and the measured data produced from *Pseudomonas fluorescens*. The red crosses are the best fit to $\delta^{15}N^{\alpha}$. The green crosses are the average best fit to $\delta^{15}N^{\alpha}$ and $\delta^{15}N^{\beta}$, hence the used values. Figure A is the first replica and the one presented in the manuscript.

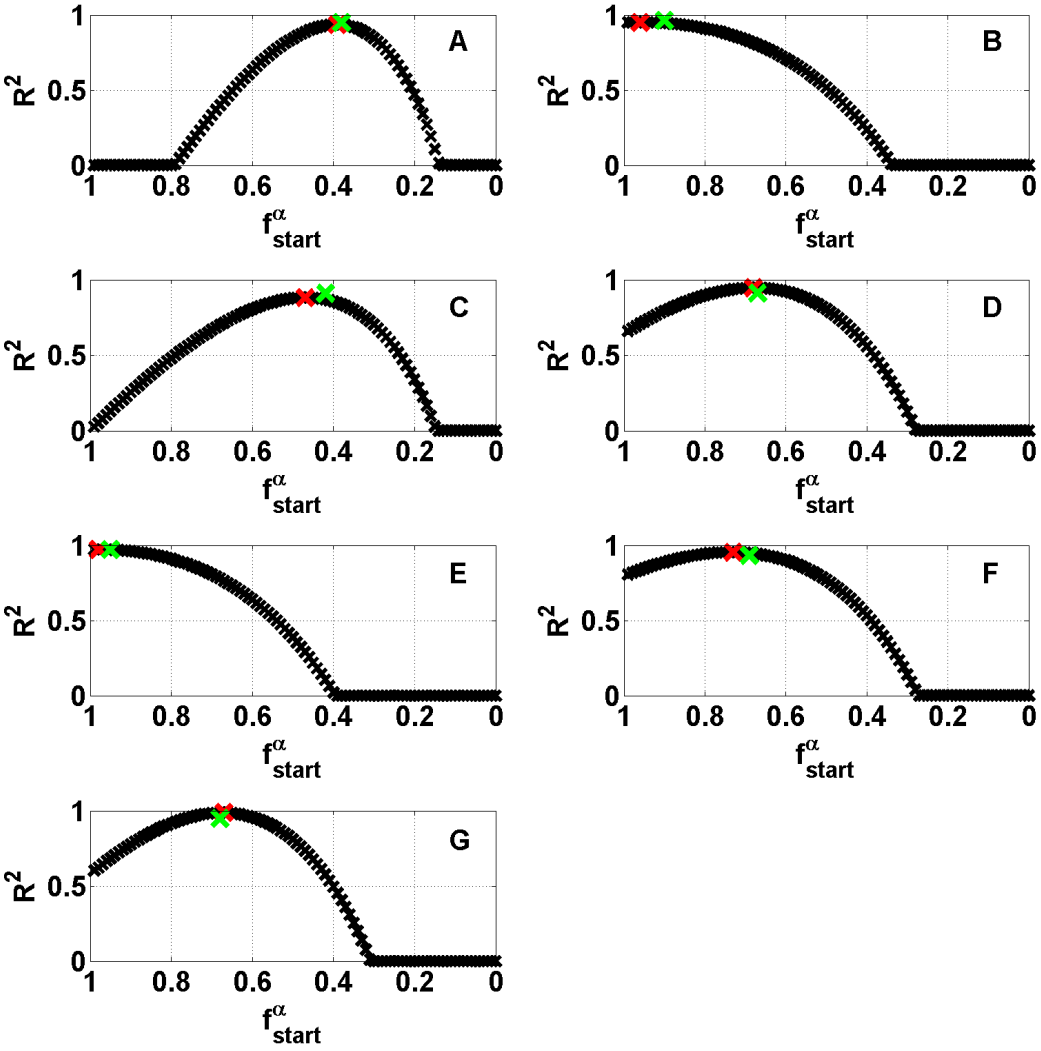

1.3.2 Figures of f_{start} for $\delta^{15}N^{\beta}$

Figures of the iterative determination of the starting point of the unreacted fraction (f) of $\delta^{15}N^{\beta}$ versus the calculated R-squared value. The black crosses are all possible f-values used in calculation of R^2 between the Rayleigh fractionation profile and the measured data produced from *Pseudomonas fluorescens*. The red crosses are the best fit to $\delta^{15}N^{\beta}$. The green crosses are the average best fit to $\delta^{15}N^{\alpha}$ and $\delta^{15}N^{\beta}$, hence the used values. Figure A is the first replica and the one presented in the manuscript.

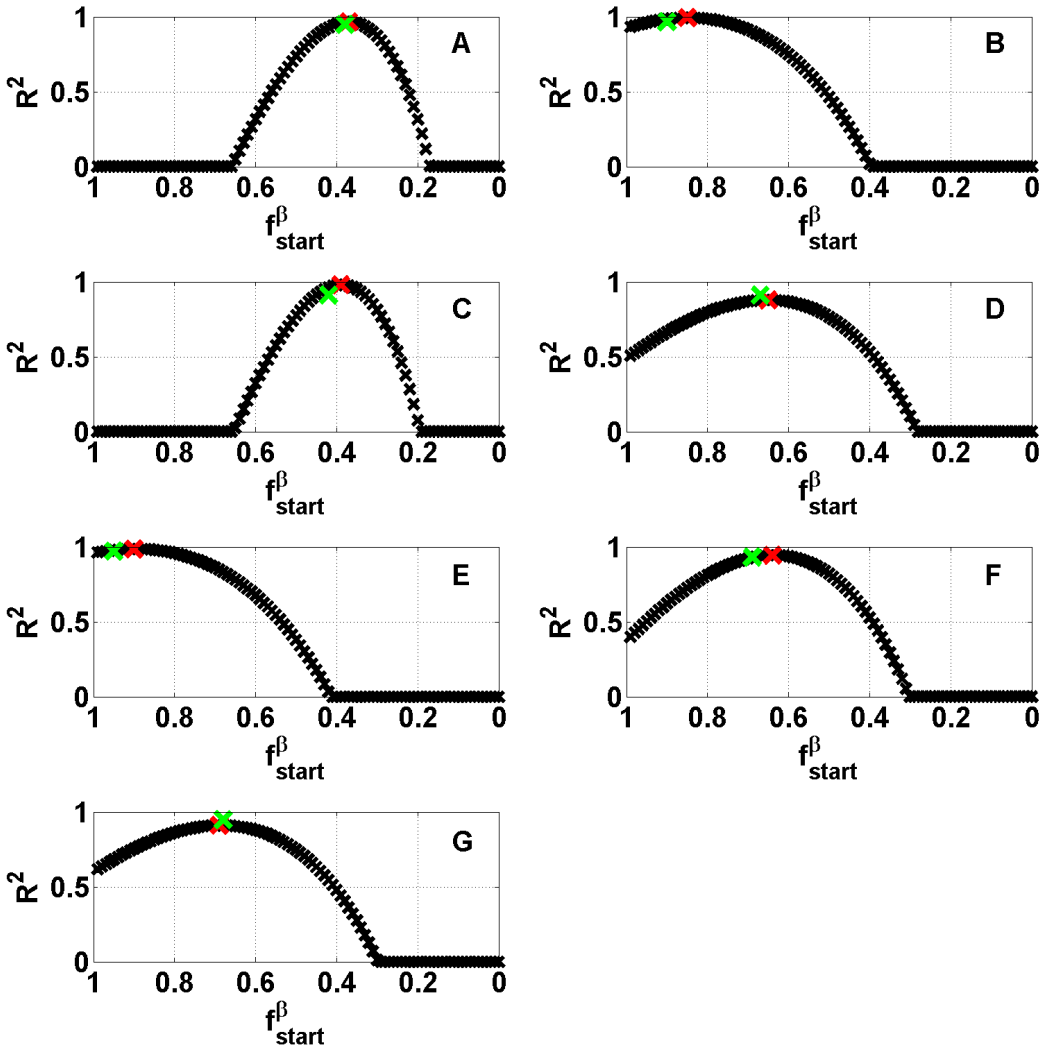

1.3.3 Figures of f_{end}

Figures of the iterative determination of the ending point of the unreacted fraction (f) versus the calculated R-squared value. The black crosses are all possible f-values used in calculation of R^2 between the Rayleigh fractionation profile and the measured data produced from *Pseudomonas fluorescens*. The green crosses are the best fit to $\delta^{15}N^{\alpha}$ and $\delta^{15}N^{\beta}$, hence the used values. Figure A is the first replica and the one presented in the manuscript.

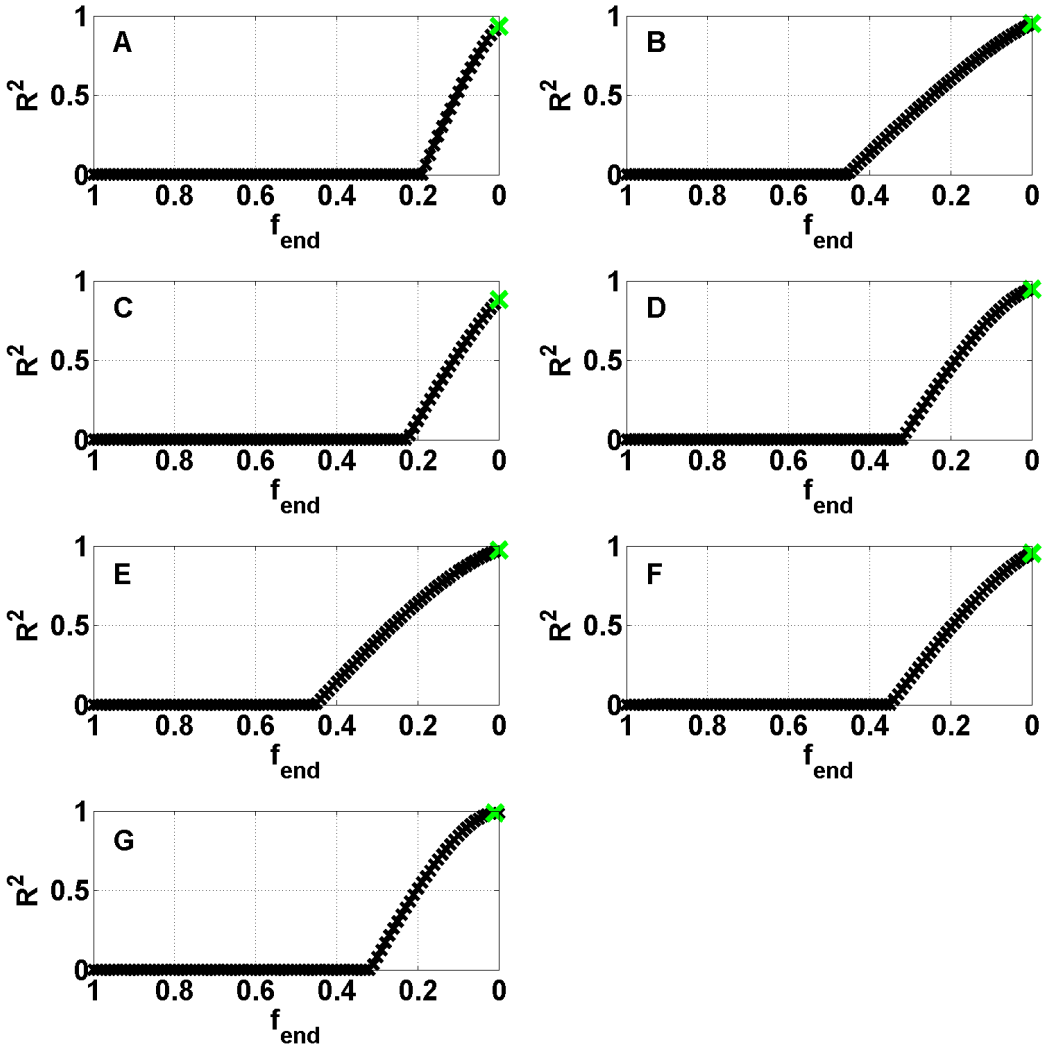

1.4 Iterative determination of the reduction correction parameter (γ)

Figures of the iterative determination of the starting point of the reduction correction parameter (γ) versus the calculated R-squared value. The black crosses are all possible γ-values used in calculation of R^2 between the Rayleigh fractionation profile and the measured data produced from *Pseudomonas fluorescens*. The green crosses are the best fit to $\delta^{15}N^{\alpha}$ and $\delta^{15}N^{\beta}$, hence the used values. Figure A is the first replica and the one presented in the manuscript.

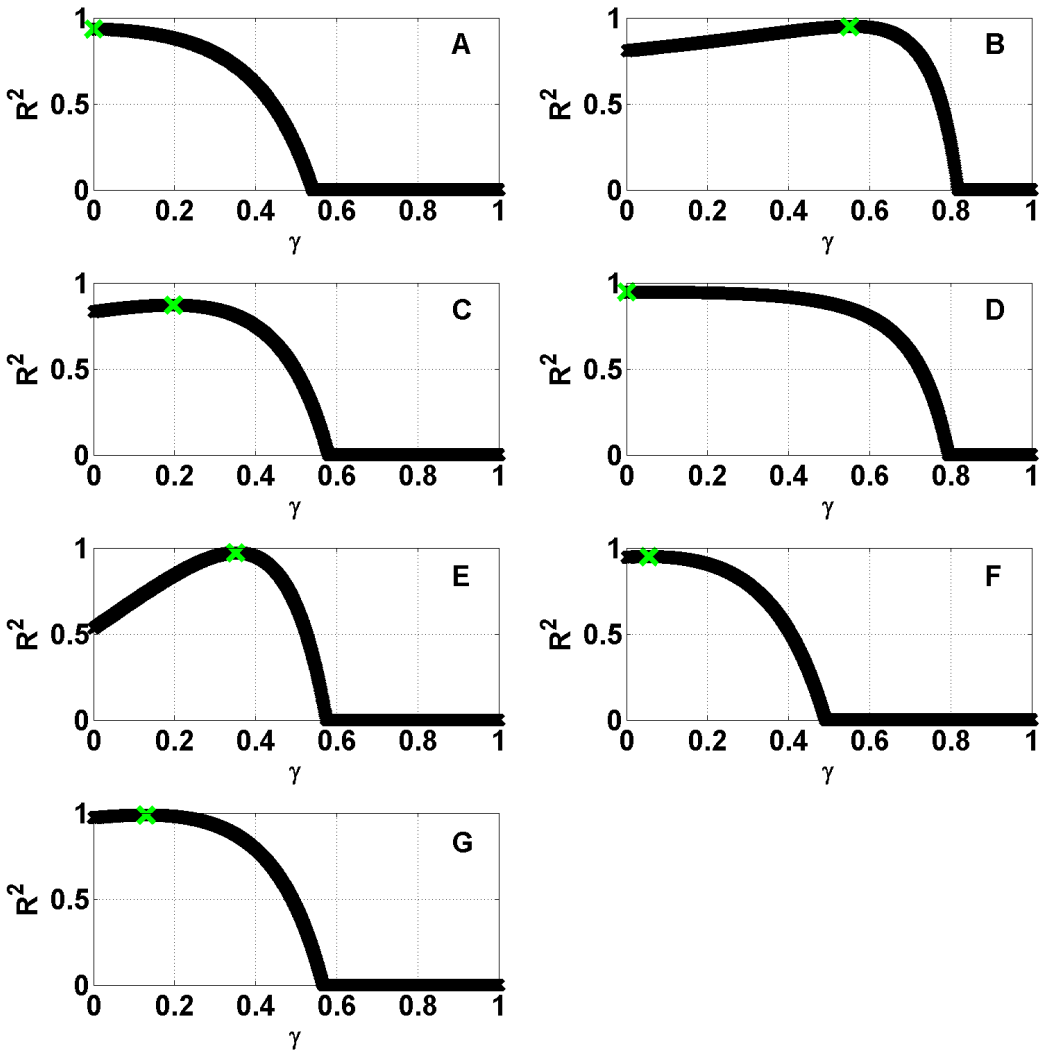

1.5 Pseudomonas Chlororaphis

1.5.1 Figures of $\delta^{15}N^{\alpha}$

Figures of the continuous measurements of the evolution of $\delta^{15}N^{\alpha}$ versus the concentration of N_2O. The blue profile is the raw production part. The black profile is the five minutes running mean of the raw measurements. The red is the fitted Rayleigh distillation for the production part. Figure A is the first replica and the one presented in the manuscript.

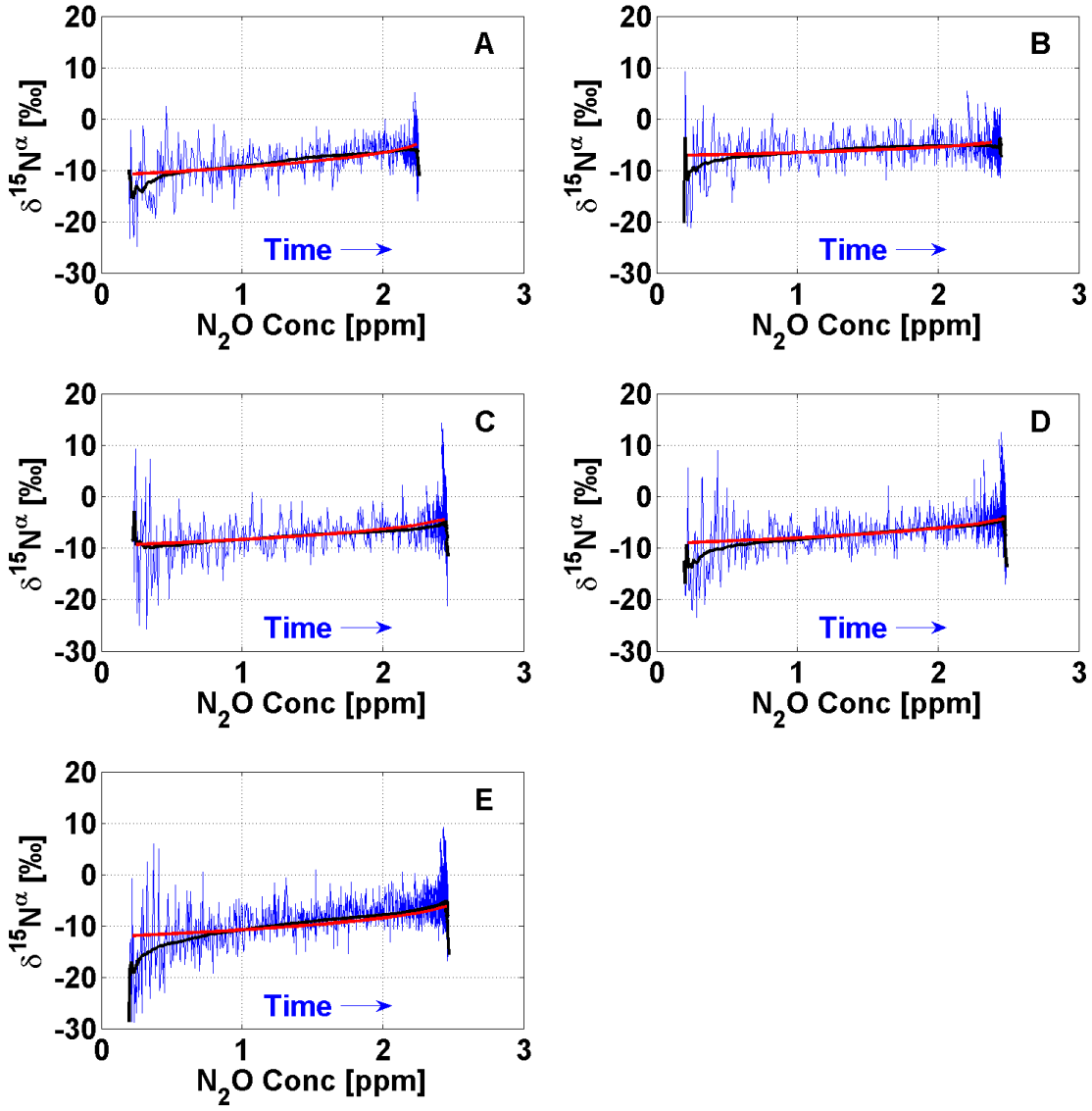

1.5.2 Figures of $\delta^{15}N^{\beta}$

Figures of the continuous measurements of the evolution of $\delta^{15}N^{\beta}$ versus the concentration of N_2O. The blue profile is the raw production part. The black profile is the five minutes running mean of the raw measurements. The red is the fitted Rayleigh distillation for the production part. Figure A is the first replica and the one presented in the manuscript.

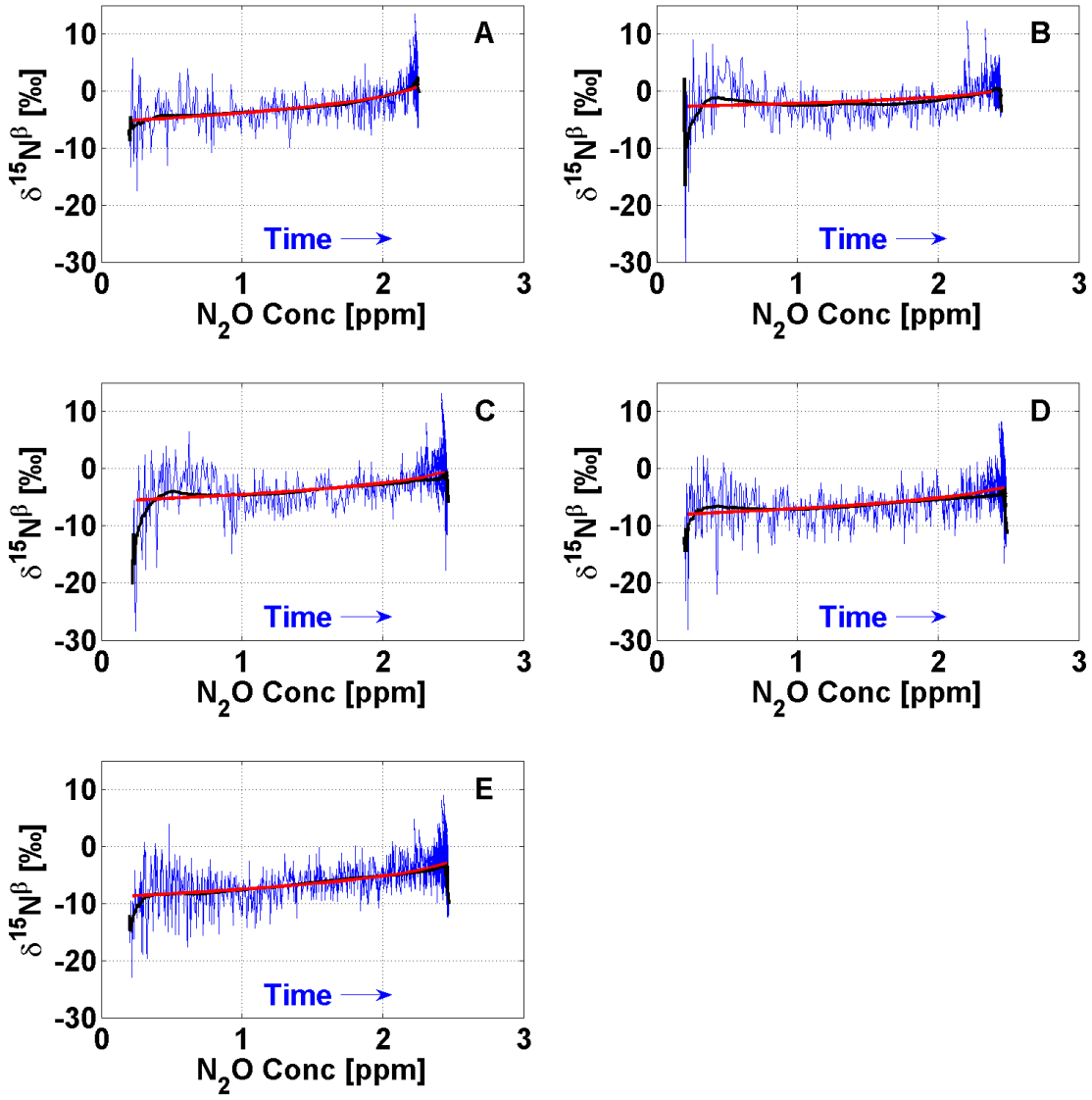

1.5.3 Figures of $\delta^{15}N^{bulk}$

Figures of the continuous measurements of the evolution of $\delta^{15}N^{bulk}$ versus the concentration of N_2O. The blue profile is the raw production part. The black profile is the five minutes running mean of the raw measurements. The red is the fitted Rayleigh distillation for the production part. Figure A is the first replica and the one presented in the manuscript.

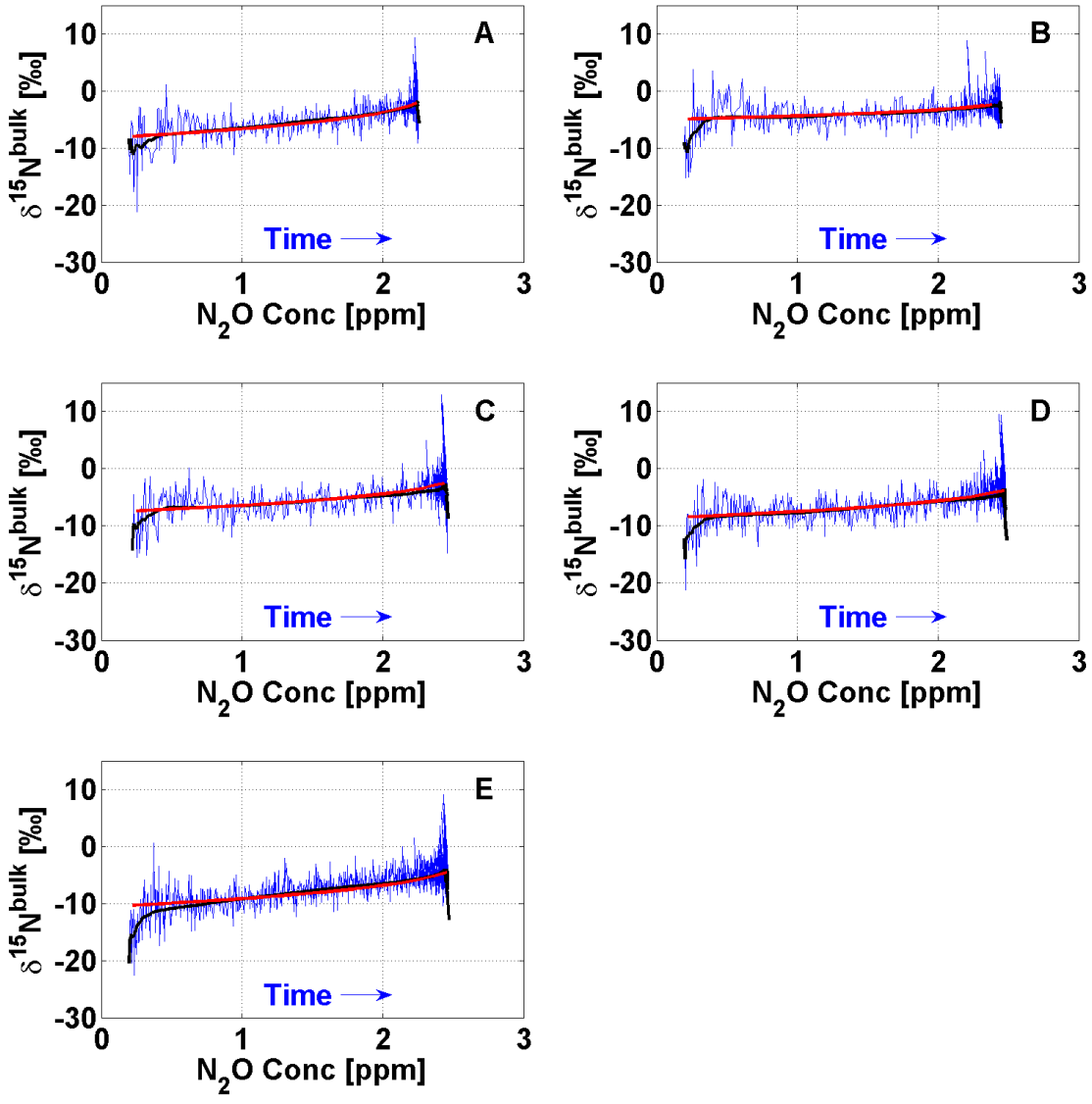

1.5.4 Figures of SP

Figures of the continuous measurements of the evolution of SP versus the concentration of N_2O. The blue profile is the raw production part. The black profile is the five minutes running mean of the raw measurements. Figure A is the first replica and the one presented in the manuscript.

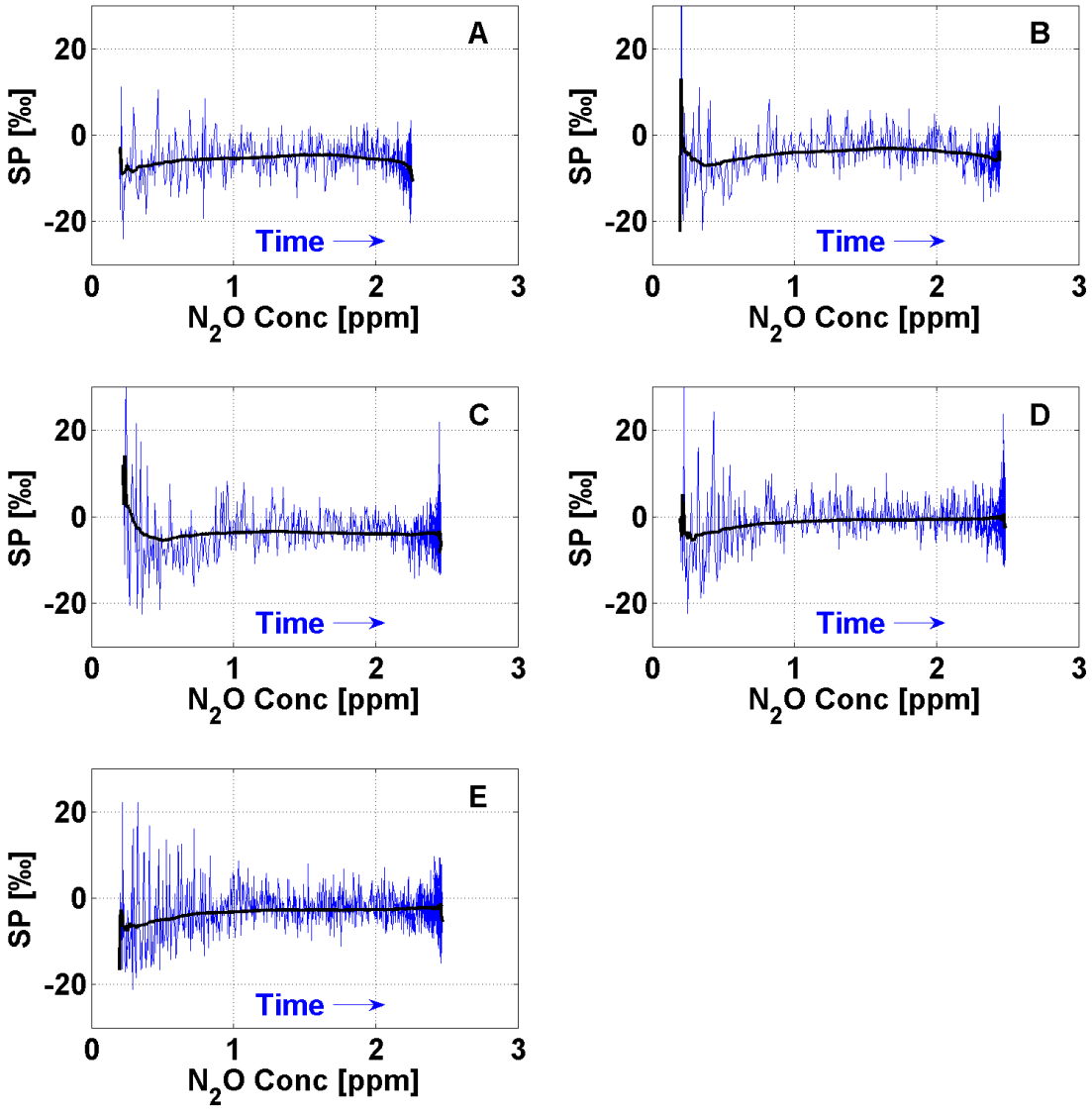

1.6 Pseudomonas Fluorescens

1.6.1 Figures of $\delta^{15}N^{\alpha}$

Figures of the continuous measurements of the evolution of $\delta^{15}N^{\alpha}$ versus the concentration of N_2O. The blue profile is the raw production part. The green profile is the raw consumption part. The black profile is the 5 minutes running mean of the raw measurements. The red is the fitted Rayleigh distillation for the production part. The magenta is the fitted Rayleigh distillation for the consumption part. Figure A is the first replica and the one presented in the manuscript.

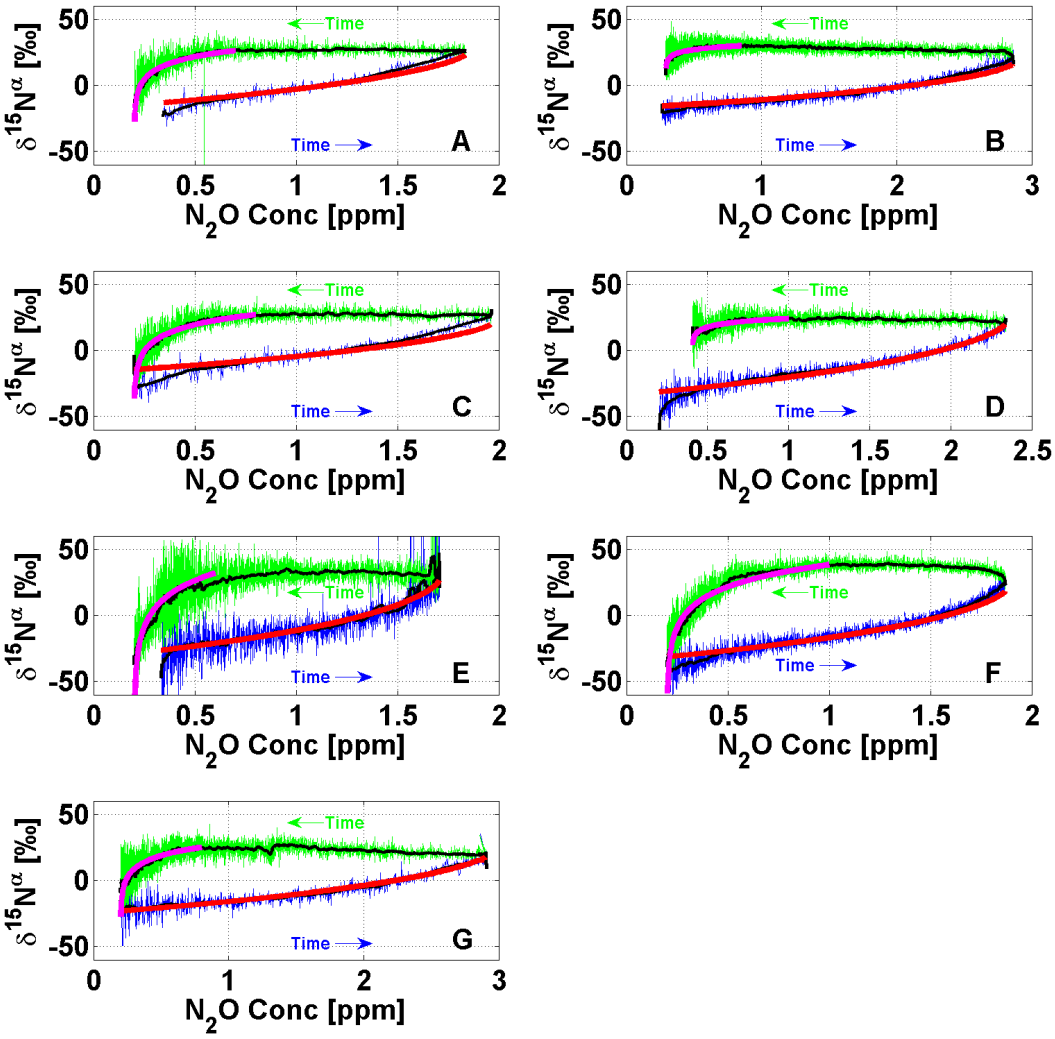

1.6.2 Figures of $\delta^{15}N^{\beta}$

Figures of the continuous measurements of the evolution of $\delta^{15}N^{\beta}$ versus the concentration of N_2O. The blue profile is the raw production part. The green profile is the raw consumption part. The black profile is the five minutes running mean of the raw measurements. The red is the fitted Rayleigh distillation for the production part. The magenta is the fitted Rayleigh distillation for the consumption part. Figure A is the first replica and the one presented in the manuscript.

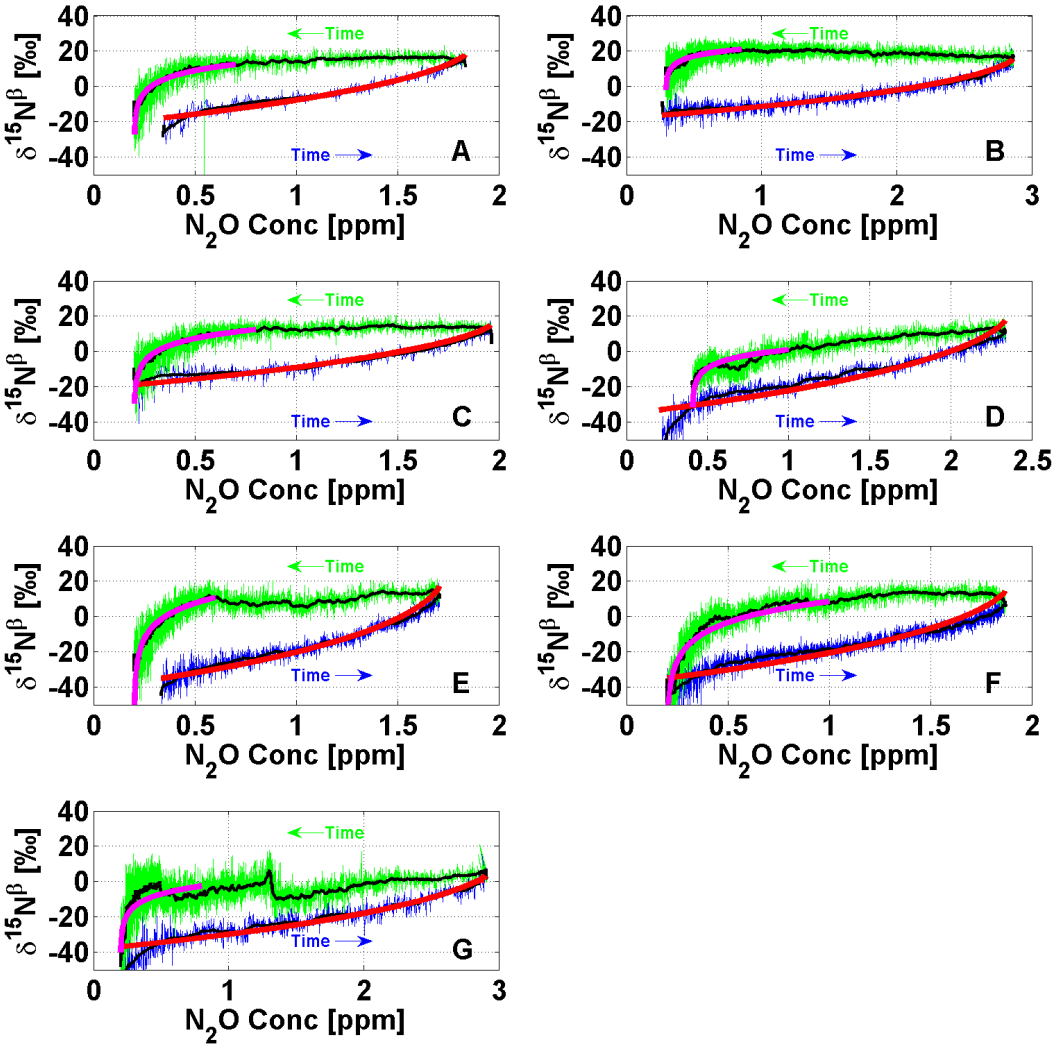

5

1.6.3 Figures of $\delta^{15}N^{bulk}$

Figures of the continuous measurements of the evolution of $\delta^{15}N^{bulk}$ versus the concentration of N_2O. The blue profile is the raw production part. The green profile is the raw consumption part. The black profile is the five minutes running mean of the raw measurements. The red is the fitted Rayleigh distillation for the production part. The magenta is the fitted Rayleigh distillation for the consumption part. Figure A is the first replica and the one presented in the manuscript.

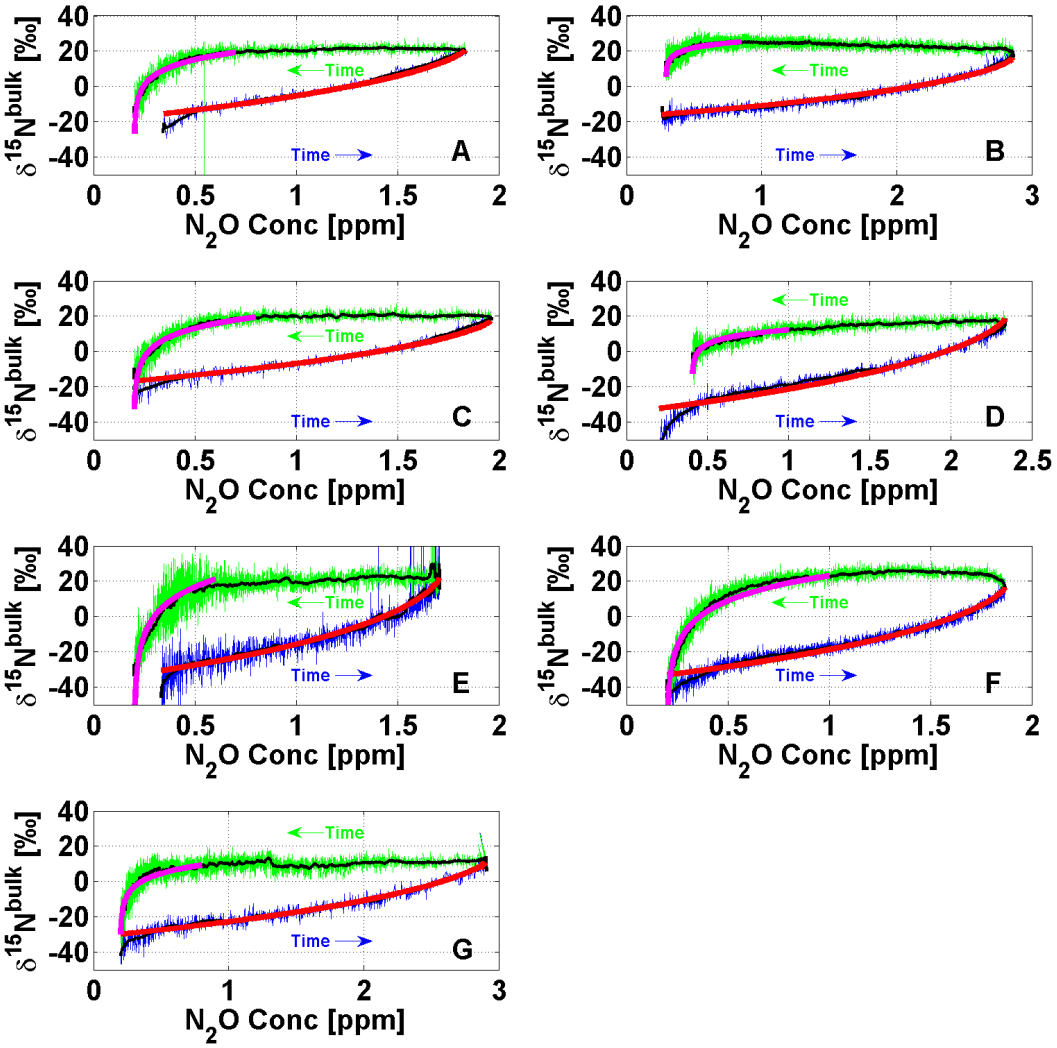

1.6.4 Figures of SP

Figures of the continuous measurements of the evolution of SP versus the concentration of N_2O. The blue profile is the raw production part. The green profile is the raw consumption part. The black profile is the five minutes running mean of the raw measurements. Figure A is the first replica and the one presented in the manuscript.